EXIT FLOW FROM A TRANSONIC COMPRESSOR ROTOR

by

William T. Thompkins, Jr.
and
Jack L. Kerrebrock

GTL Report No. 123 September 1975

GAS TURBINE LABORATORY
MASSACHUSETTS INSTITUTE OF TECHNOLOGY
CAMBRIDGE, MASSACHUSETTS

EXIT FLOW FROM A TRANSONIC COMPRESSOR ROTOR

by

William T. Thompkins, Jr.
and
Jack L. Kerrebrock

GTL Report No. 123 September 1975

This research was supported in part by the NASA Lewis Research Center under Grant NGL 22-009-383, Pratt & Whitney Aircraft Division, United Technology Corporation, and the General Electric Company.

EXIT FLOW FROM A TRANSONIC COMPRESSOR ROTOR

by
William T. Thompkins, Jr.
Research Assistant
Gas Turbine Laboratory
and
Jack L. Kerrebrock
Professor of Aeronautics and Astronautics
Director, Gas Turbine Laboratory
Massachusetts Institute of Technology
Cambridge, Massachusetts 02139
USA

SUMMARY

The three dimensional unsteady flow field behind a transonic compressor rotor with a design pressure ratio of 1.6 at a tip Mach number of 1.2 has been resolved on the blade-passing time scale, using the M.I.T. Blowdown Compressor Facility. Quantities determined were total and static pressures, tangential flow angle and radial flow angle. The spatial and temporal resolution achieved was sufficient to determine velocity components inside individual blade wakes and in the surrounding flow. From these measurements the flow structure is described at stations immediately behind the rotor and one chord downstream. Some dominant features of the flow just behind the rotor are large radial velocity components, large static pressure fluctuations near the blade wakes, and definite unsteadiness (in rotor coordinates) of the wakes. The wake behavior one chord downstream is described in terms of the effect of the strong mean swirl on the behavior of shear disturbances. In the outer portion of the annulus, where the mean flow approximates a solid body rotation, a strong, persistent oscillatory flow is found with 16 periods in the circumference as roughly predicted by theory. In the inner portion of the annulus the disturbances attenuate axially.

INTRODUCTION

The flow through high work compressors deviates from the idealized model of a nearly two dimensional flow along cylindrical stream surfaces because of a number of phenomena including vorticity shedding due to spanwise circulation variations, radial flow in the boundary layers, variations in passage shock strength, casing boundary layer growth, and more. An understanding of the flow field induced by these phenomena seems essential to progress in reducing the losses in such rotors.

This paper reports some results of a comprehensive investigation of the flow through such a high work transonic compressor rotor, being conducted at the M.I.T. Gas Turbine Laboratory. The immediate objectives of the program include a thorough experimental investigation of the flow ahead of, within, and downstream of the rotor, and development of theoretical models capable of describing the flow quantitatively. In the present paper two aspects of the study will be discussed; a detailed time resolved study of the flow field downstream of the rotor, and a linearized description of the flow field accounting for the strong mean swirl.

At present, few detailed measurements are available within the rotor passage; Epstein[1] has obtained quantitative density maps by gas fluorescence in the same rotor studied here, as a part of this comprehensive program. Very few measurements have been carried out downstream of rotors. Reference (2) presents downstream data for a low speed rotor, but the data to be given here are probably the first obtained for a high work, transonic compressor. The rotor has a tip Mach number of 1.2, a design pressure ratio of 1.6, and inlet hub/tip ratio of 0.5. Time resolved measurements of static pressure, stagnation pressure, and the axial, tangential and radial components of Mach number will be presented for two axial stations downstream of the rotor.

As an aid to understanding these complex results, a general theory of small disturbance fields in strongly rotating flows has been developed[3] and some qualitative features of the results will be compared to the data.

The authors have considerable confidence in the experimental results and feel they are representative of the behavior of many useful transonic rotors. They are complex, and full understanding of their implications is not claimed. The interpretation through the linearized disturbance theory is tentative, and but a first step at best.

EXPERIMENTS

Test Facility

The experiments described in this paper were conducted in the M.I.T. Blowdown Compressor Facility. This facility and the test rotor are described in detail in Ref. (4). Essentially, the facility provides means for testing a two-foot diameter transonic rotor in a pulsed mode, with a test time of about 30 milliseconds during which the rotor is driven by its angular inertia, and operates at fixed axial and tangential Mach numbers. Measuring probes can be surveyed over the span during this test time, at a number of axial stations. A schematic of the test section and rotor flow path are given in Fig. 1.

Instrumentation

Time resolved measurements of the fluctuating pressures behind the compressor rotor were determined using probes based on the miniature silicon-bonded transducers produced by the Kulite Corporation. These

transducers have frequency response flat from DC to 100 kHz and their diameter is 1.5 mm. Probes which can be used to resolve highly unsteady three dimensional flow fields can be produced by combining several of these diaphragms into one probe body. The probe design used for these experiments is shown in schematic form in Fig. 2. Four transducers were mounted on flats on a cylindrical body to construct this probe. One transducer faces the mean flow direction while the remainder are inclined at ±45 degrees to the mean flow direction. During a compressor test the probe is traversed radially inward with transducer number 1 perpendicular to the mean flow direction.

The fraction of the free stream dynamic pressure recovered at each transducer location is primarily a function of radial and pitchwise flow angles. Dynamic pressure recovery is influenced to a much lesser degree by Mach number and Reynolds number. The pressure recovery measured at each transducer location during steady state testing is shown in Figs. 3a, b, and c for several combinations of flow angles. The recovery measured for transducer number 2, which is not shown, is identical to that of transducer number 3, if the sign of θ is reversed. During a compressor test the transducers are referenced to vacuum and thus indicate absolute pressure. An iterative procedure is used to determine the freestream total pressure, static pressure, radial flow angle, and pitchwise flow angle which would be compatible with the four measured pressures using these probe calibrations.

The effect of Mach number and Reynolds number variation on the probe calibrations were determined in steady state model testing. The range of Mach number simulated was 0.25 to 0.55; the range of Reynolds number simulated was 0.8×10^4 to 3×10^4, based on probe diameter. The effect of changing Mach number and Reunolds number over these ranges was small for angle variations of ±15 degrees. For larger angle variations the effects of Mach number and Reynolds number are expected to be much stronger.

The physical dimensions of the traversing probe limit the spatial resolution that may be achieved. For the rotor tested the pitchwise distance between transducers is about 3% of blade spacing at the hub; while in the radial direction the maximum distance between transducers is about 5% of the blade span. Large flow gradients cannot be reliably determined over distances smaller than these.

It should be noted that the transducers are mounted on the probe body without any surrounding cavities. In this way the full frequency response of the transducers is retained. However the flow time across these transducers limits the probe response to about 10 times blade passing frequency, which is sufficient to resolve events occurring in the blade passing time scale.

Data Reduction

During a compressor test high response data is recorded on a 14-channel-wide band FM tape recorder with a frequency response from DC to 80 kHz at 120 in. per second tape speed. One channel is reserved for an internal oscillator (200 kHz) which gives an absolute time base for the experiment. For later analysis each tape recorder channel is played back, with tape recorder speed reduced by a factor of 64, simultaneously with the internal oscillator into a two-channel analog to digital converter. The converter produces a magnetic tape which may then be processed at the M.I.T. Information Processing Center. Required calibration procedures are applied to convert the digital voltages into pressure values. The four digitized pressure measurements from the traversing probe are used to determine the freestream conditions at all times during the probe traverse. This data may then be randomly retrieved for examination.

A problem which has often interfered with measurements of absolute pressures using the Kulite transducer is that of long-term thermal drift. This problem is mitigated by the extremely short test time and by calibration against thermally stable low frequency transducers during a rotor test.

Results

In order to map out the flow field downstream of the test rotor, time resolved pressure measurements were recorded during radial surveys at two axial stations, 0.1 chords downstream and 1.0 chords downstream. Since the rotor pressure distribution is swept past the traversing probe much faster than the probe is moved radially, a complete map of the flow field in one radial plane can be determined during one test run.

Measurements typical of those recorded when the probe was at $r/r_t = 0.74$ and 0.1 chords downstream are shown in Figs. 4a, b, and c. Figure 4a shows the total pressure ratio (P_{t2}/P_{t1}) and the static pressure ratio (P_{s2}/P_{t1}); Figs. 4b and c show the Mach number components as computed from pressures plus the measured flow angles. As time increases in these plots, the rotor turns such that the probe appears to move from the suction side of one blade to the pressure side of the adjacent blade.

Some of the features of the traditional model of an inviscid core flow plus a viscous wake appear in this data. Figure 4b shows the axial and pitchwise Mach number profiles of a clearly defined viscous wake embedded in a more or less constant Mach number flow.

But the static pressure is not uniform across this wake, as can be seen from Fig. 4a, in fact it varies by as much as plus and minus 25 percent, so that the viscous "wake" should not be expected to behave in the traditional way. Close scrutiny of Figs. 4a and 4b shows that the peaks of static pressure (and also of stagnation pressure) lie outside the "wake" region, with a minimum of pressure on the pressure side of the blade and a maximum on the suction side.

A further difference from the traditional picture lies in the large radial Mach number (up to 0.25), which can be seen from Fig. 4c to exist at the tangential location of minimum static pressure, i.e. on the pressure side of the "wake."

Similar data which were recorded when the traversing probe was located at $r/r_t = 0.87$ are shown in Fig. 5. These data, which are representative of results obtained at high r/r_t, are quite different from the previous results. Considerable blade to blade variation exists and no clear separation into an inviscid core flow plus a viscous wake appears. Very large radial flows, of the same order as the axial flow, occur in the flow field.

These two radii, r/r_t = 0.738 and 0.870, roughly straddle the nominal sonic radius of the rotor. Epstein has found by the fluorescent density measurement technique evidence of an unsteady separation process at r/r_t = 0.83, which is again in this range. This data will be presented in Ref. (5), which is in preparation.

It should be remarked here that radial or pitchwise flow angles relative to the probe larger than ±20 degrees are beyond the limits where consistent calibrations of the probe pressure recovery were obtained. For the data described above a ±20 degree variation in pitchwise flow angle relative to the probe corresponds to absolute flow angles of 25 to 65 degrees. Data falling outside these ranges must be considered as only approximations to the true flow.

As was previously stated, large blade-to-blade variations exist for $r/r_t > 0.80$; moreover, by examining the wakes shed by a single blade during successive passes at a constant r/r_t, it was found that the flow is quite unsteady in rotor coordinates. For $r/r_t < 0.80$ the flow appears to be steady in rotor coordinates.

Time averages of selected flow variables were computed for two radial surveys, 0.1 chords downstream of the rotor and 1.0 chords downstream of the rotor. These averages were computed from data samples 5 blade passing periods in length. The average total pressure ratio is shown in Fig. 6a. Its value closely approaches the design value of 1.6. Average pitchwise and axial Mach numbers are shown in Figs. 6c and 6d. Considerable deviations from the design profiles exist especially at larger r/r_t. The time averaged radial Mach number was approximately zero at all radii.

An average total temperature ratio was determined using Euler's equation and is shown in Fig. 6b along with the isentropic temperature ratio determined from the measured total pressure values. At low r/r_t a local efficiency would be very high as might be expected from the type of flow shown in Fig. 4. At larger r/r_t a local efficiency would be very poor as would be expected from a flow like that of Fig. 5. There is a systematic difference between the stagnation pressures at station 5 and those at station 6, which corresponds to approximately a 4 percent decrease in efficiency, based on time-averaged stagnation pressure and temperature. This represents the efficiency loss due to wake mixing between stations 5 and 6.

Whenever high response data is collected, a serious problem arises in assimilating the quantity of data recorded. Our attempt to overcome this problem is to construct level curves or contour plots of flow variables in the r-θ plane. Data samples recorded at several radial positions and approximately 3 blade passing periods in length were selected. The samples were all chosen to begin at the same relative time in a blade passing period. A data point in these samples then corresponds to a point in a sector of the r-θ plane including 3 blade passages.

A contour plot of the rotor total pressure in the radial plane 0.1 chords downstream of the rotor is shown in Fig. 7a. In this plot data from 10 radial positions were used. The time average value of total pressure ratio is 1.62. At small r/r_t the flow field can be seen to have nearly constant total pressure except near the blade wakes. Around midspan islands of high pressure appear in the core flow as well as near the wakes. At large r/r_t numerous islands of high and low pressure are scattered throughout the flow field.

It should be emphasized that these data are in a sense taken out of context since data from several different physical blades are combined into a single plot. As was previously discussed, unsteadiness does exist and is important at larger radii; therefore some distortion and loss of detail in these contour plots is unavoidable. However, flow features common to all blades will be emphasized by this procedure.

A contour plot of the rotor static pressure ratio (P_{s2}/P_{t1}) is shown in Fig. 7b. Many interesting features appear in this plot; in particular the high static pressure area at about midspan and the local high gradient low pressure area. No convincing explanation for the origin of these areas is yet known; however, the existence of these areas is supported by the intra-blade density measurements performed by Epstein[5], as noted above.

To aid in determining the losses and the distribution of these losses a calculation of the local total temperature ratio and from it the local entropy rise across the rotor was attempted. For this test rotor, which has no upstream swirl, Euler's turbine equation has a simple form and was used to calculate the local total temperature. When the local total temperature ratio and total pressure ratio are known, the entropy rise across the rotor may be determined. This approach will be strictly valid for those streamtubes for which the flow in the relative coordinate system is steady; for other streamtubes the procedure will yield only approximate results. A contour plot of the entropy rise, $(S_2-S_1)/C_v$, is shown in Fig. 7c. At low r/r_t the flow appears to be very nearly isentropic except for the wakes. above midspan isolated regions of high entropy appear.

Contour maps of the axial Mach number, pitchwise Mach number, radial Mach number and total temperature ratio are included as Figs. 7d, e, f, g, and h for later reference.

These data all appear to be self-consistent. For example, large radial flows are directed away from the high static pressure areas at about midspan. In addition, these data all have large disturbances concentrated at blade passing frequency.

A similar set of contour plots was prepared from the radial survey done 1.0 chords downstream of the rotor and are shown in Figs. 8a, b, c, d, and e. These figures show that considerable evolution of the flow field occurs between the two radial survey locations. In particular, considerable decay of the disturbances introduced by the rotor has occurred at smaller r/r_t, while at larger r/r_t the disturbances seem to have propagated without significant decay. In addition, the disturbance frequency for $r/r_t > 0.82$ seems to be significantly lower than the blade passing frequency. These trends will be discussed more completely in the next section, in conjunction with the small disturbance theory.

THEORETICAL CONSIDERATIONS

To the extent that the flow behind the compressor rotor may be thought of as an axisymmetric steady base flow perturbed by an unsteady θ dependent disturbance field, it should be representable by a linear theory based on an expansion about the axisymmetric throughflow. One approach to such a theory is to determine the duct eigenfunctions which satisfy the differential equations resulting from such an expansion, and which also satisfy the boundary conditions at the hub and tip diameters, and to then attempt to match a set of such eigenfunctions to the disturbance produced by the blade row. In first approximation, the disturbances can be described by an inviscid heat conduction-free model, because the Reynolds number of the disturbances is large once they leave the blades which produced them. This is true even though viscous forces on the blades are the controlling factor in producing the disturbances. Of course some of the disturbances of interest arise from inviscid phenomena, such as spanwise circulation variations, but the main focus here will be on those of viscous origin, as they appear to dominate in the Blowdown Compressor rotor. A first attempt at such an approach has been described in Ref. (3). The present discussion will draw on that work and further developments along the same lines to help explain the experimental results described above.

The most important feature of the mean flow downstream of the rotor is its strong rotation. Ideally, this would approach a free vortex; in practice it is more nearly a constant swirl-angle flow, and for the present purposes it will be approximated by a tangential velocity distribution, $V = \Omega r + \Gamma/r$. Now it is well known[6] that in the absence of the rotation, i.e., in a uniform axial flow, a general small disturbance field can be represented as a sum of three separate modes consisting respectively of entropy, vorticity, and pressure fluctuations, the last having associated (irrotational) velocity and (isentropic) density and temperature fluctuations. The vorticity mode represents convected wake (shear) disturbances, while the pressure mode represents the propagating (sound) or elliptic pressure field. In contrast, for the strongly rotating fluid there are not three distinct modes, since the centrifugal forces resulting from density and tangential velocity fluctuations generate pressure disturbances, as do the coriolis forces associated with radial velocity perturbations. Thus we might expect a qualitatively different behavior for the flow downstream of a blade row from that behind a wing or body.

It is argued in Ref. (3) that the dimensionless number which measures the importance of the base rotation is a Rossby number, $\varepsilon = V/\Omega L$, where V is the local tangential velocity, Ω the local angular velocity, and L a characteristic length for the disturbance. If we think of V/L as a "disturbance frequency", then ε is the ratio of disturbance frequency to mean rotational frequency. When it is large, the fluid accelerations due to the disturbance are large compared to those due to the rotation, and we might expect the effects of rotation to be small. When the disturbance frequency is small, however, we would conversely expect the effects of the fluid rotation to be controlling. The detailed analysis of Ref. (3) shows in fact that the pressure field of a many bladed rotor is in these terms a high frequency disturbance, and that the effects of mean rotation on its behavior are minor. On the other hand, the frequency of wake disturbances would be zero (in rotor coordinates) in the nonrotating case, so we should expect the effects of mean rotation to strongly influence their behavior. The next few paragraphs will summarize the main points of the argument, in comparison to the experiment.

Following the procedure of Ref. (3) we expand the general small disturbance field about a mean flow with radially uniform entropy S and axial velocity W. The tangential velocity $V = V(r)$. We find then that entropy perturbations in this flow satisfy the relation

$$L(s) = 0$$

where

$$L \equiv \frac{\partial}{\partial \tau} + (V/r)\ (\partial/\partial\theta) + W(\partial/\partial z) \qquad (1)$$

so that they are convected by the mean flow.

Since the mean flow varies only in r, not in θ or z, the coefficients in the differential equations depend only on r, and it is natural to seek solutions for the density and velocities of the form

$$p\ (r, \theta, z, \tau) = \int p\ (r, m, k, \omega)\ \exp\ [i(kz + m\theta - \omega\tau)]\ dmdkd\omega$$

whereupon it can be shown that p is governed by a single second order differential equation. If we neglect the effect of entropy perturbations on the density and velocity, the equation becomes

$$r^2 \frac{d^2p}{dr^2} + \left(1 - \frac{rD'}{D}\right) r \frac{dp}{dr} + \left[-\frac{r^2k^2D}{\lambda^2} - m^2 - \frac{2mV}{\lambda r}\left(1 + \frac{rD'}{D}\frac{rV'}{V}\right)\right] p = 0 \qquad (2)$$

where $\lambda = kW + mV/r - \omega$ and $D = \lambda^2 - (2V/r)(V' + V/r)$,

the prime indicating differentiation with respect to r. The radial velocity is given by

$$u = \frac{i}{D}\left(\frac{\lambda}{R}\frac{dp}{dr} + \frac{2mV}{Rr^2}\,p\right) \qquad (3)$$

where R is the mean flow density, and the tangential and axial velocities are

$$v = -\frac{1}{D}\left[\frac{(V' + V/r)}{R}\frac{dp}{dr} + \frac{\lambda m}{Rr}\,p\right] \qquad (4)$$

$$w = -\frac{k}{\lambda R}\,p \qquad (5)$$

The existence of solutions of (2) satisfying the boundary conditions u = 0 at the hub and tip radii essentially requires that the solutions oscillate in r, since u is connected to p by the first order differential equation (3) and must have successively larger numbers of zeros in the annulus as the eigenvalue is increased. Writing (2) in the form of a comparison equation,

$$a(r)\,\frac{d^2p}{dr^2} + b(r)\,\frac{dp}{dr} + c(r)\,p = 0$$

shows that the local condition for oscillation is that $b^2 - 4ac < 0$, and since $a = r^2$ is positive, this requires that c be sufficiently positive. An infinite set of solutions is required to represent by superposition an arbitrary disturbance field, so c must take on successively larger positive values, giving larger numbers of oscillations within the annulus, as the eigenvalue is increased.

In the compressor annulus we can view m and ω as being specified by the boundary conditions at the rotor plane. Thus for the blade passing harmonic m = 23 for the Blowdown Compressor, while $\omega = m\Omega_R$, where Ω_R is the rotor's angular velocity. The axial wave number, k , is the eigenvalue. Its value controls those of λ, D, and the other functions which appear in the coefficients of (2).

The behavior of the solutions will be discussed for two relatively simple mean flows before turning to the actual Blowdown Compressor flow.

Non-rotating Flow

The characteristics of the solutions depend on whether k is real, complex, or pure imaginary. Turning to the case of non-rotating flow as a first illustration, there would be three classes of disturbances. For convected vorticity and entropy $\lambda = 0$, so $k = \omega/W = m\Omega_R/W$ is real. For nonpropagating (elliptic) pressure disturbances $k = \pm ik_I$, a pair of pure imaginary values corresponding to exponential decay in z away from the source. For sound disturbances $k = \lambda/W + m\Omega_R/W$, where now λ is of order $m\Omega_R$, so k is again real, but such propagating pressure waves are excited only if the source has supersonic velocity relative to the fluid.

Wheel Flow

Since the relative outflow from the Blowdown Compressor rotor is subsonic, we will consider the rotating fluid analogs of only the first two types of disturbances. This justifies an incompressible treatment, wich has been assumed in Eq. (2). Now for $V = \Omega r$, $\lambda = kW + m\Omega - \omega$ is constant, $D = \lambda^2 - \Omega^2$ is also constant, and the equation becomes simply

$$r\,\frac{d^2p}{dr^2} + r\,\frac{dp}{dr} + \left[\frac{-r^2k^2(\lambda^2 - 4\Omega^2)}{\lambda^2} - m^2\right]p = 0 \qquad (6)$$

It is readily seen that solutions with real k, i.e., oscillatory in z, will exist for $\lambda^2 < 4\Omega^2$, since then c(r) can be arbitrarily positive for λ^2 sufficiently small. We note that since λ is the frequency of the disturbance in a coordinate system moving with the fluid, $(\lambda/2\Omega)$ is the ratio of disturbance frequency to fluid rotational frequency (apart from a factor of 2). From this we conclude that there is an infinite set of nearly convected (i.e., low frequency) disturbances, which are the analogue of vorticity in uniform flows. The characteristics of such disturbances shed from inlet guide vanes into a wheel flow have been presented in Ref. (3) and studied in detail by Yousefian[7].

These "shear waves" propagate relative to the mean flow. As an example, take a case of $\lambda/\Omega = \pm 1/2$. then

$$\frac{kW}{\Omega} = \frac{\lambda}{\Omega} - m + \frac{\omega}{\Omega} = \pm\frac{1}{2} - m + \frac{\omega}{\Omega}$$

For the Blowdown Compressor take m = 23, and $\omega/\Omega = m\Omega_R/\Omega \simeq 23(5) \simeq 125$, so $kW/\Omega \simeq 100 \pm 1/2$. The value $kW/\Omega = 100$ corresponds to pure convection for this case, so we would have a pair of waves splitting very slightly from the convective direction. Note that the splitting would be much stronger for small m; for m = 1, $kW/\Omega = 4 \pm 1/2$. Of course this example is not directly relevant to the experiment because the flow behind the rotor is not a wheel flow.

If $(\lambda^2) >> \Omega^2$, c(r) becomes independent of Ω and $c \propto k^2$, so that c can be arbitrarily positive for $k = \pm ik_I$, and k_I large. These eigenfunctions represent the elliptic pressure disturbances, being harmonic in θ and τ, but attenuated in z.

Some comments about the velocity field are in order for this relatively simple case. Since k and λ are real for the shear waves ($\lambda^2 < 4\Omega^2$), p, v, and w are all in phase, while u is shifted $\pi/2$ in $m\theta$. That p is in phase with v and w allows an energy flux in the wave perpendicular to the rotor plane, hence a propagation in z. For the elliptic pressure disturbances, where $k = \pm ik_I$, $\lambda = \pm ik_IW + m\Omega - \omega$ is complex, and the situation is also more complex, but it is readily seen that p and w are shifted in phase relative to v.

Rotor Exit Flows

We take $V = \Omega r + \Gamma/r$ as a model for the flow behind the Blowdown Compressor rotor, so that $\lambda = kW + m\Omega - \omega + m\Gamma/r^2$ is a function of r. But the condition for existence of multiple solutions of (2) is still that the term $-r^2k^2D/\lambda^2$ take on sufficiently large positive values, since the other terms vary comparatively weakly with λ. As for the wheel flow, there are two classes of solutions. For "high frequency" disturbances, $D/\lambda^2 \to 1$, and the behavior is controlled by $-k^2$, so that we find $k \simeq \pm ik_I$ as before, and such high frequency disturbances are elliptic, i.e. attenuated in z with relatively minor effects of rotation.

For "low frequency" disturbances we will have oscillatory behavior in z when D/λ^2 is sufficiently negative, otherwise k will be complex or imaginary. Consider first the oscillatory case. Then

$$\frac{D}{\lambda^2} = 1 - \frac{4(1 + \Gamma/\Omega r^2)}{(\lambda/\Omega)^2} = 1 - \frac{4}{m^2} \frac{(1 + \Gamma/\Omega r^2)}{(\lambda_o/m\Omega + \Gamma/\Omega r^2)^2}$$

must be sufficiently negative to produce the required oscillations, where $\lambda_o = kW + m\Omega - \omega$. From (3) it is clear that D may not have a zero in the turbomachine annulus (unless it is cancelled by a zero of the bracketed term), so tentatively we refine this condition to the requirement that

$$\frac{-m\Gamma}{\Omega r^2} - 2\sqrt{1 + \frac{\Gamma}{\Omega r^2}} < \frac{\lambda_o}{\Omega} < -\frac{m\Gamma}{\Omega r^2} + 2\sqrt{1 + \frac{\Gamma}{\Omega r^2}} \qquad (7)$$

for oscillatory solutions with real k. The tendency toward oscillation should be strongest for the value of r where $\lambda_o = -m\Gamma/r^2$, i.e., for $\lambda = \lambda_o + m\Gamma/r^2 = 0$. This radius will be termed the "convection radius", r_c.

The regions of oscillatory behavior are plotted vs. $\Gamma/\Omega r^2$ for two values of m in Fig. 9, from which it is clear that the range of $\Gamma/\Omega r^2$ for oscillatory behavior becomes very narrow for large m, but is broad for small m. Thus, we conclude that

a) small m disturbances are more likely to be oscillatory (persistent) in the downstream flow than those with large m.

In the event that no solutions exist for real k, as is likely for large m because D/λ^2 is not negative over a sufficient range of r, then k must be complex or imaginary. If we ignore the λ in the last term, Eq. (2) depends only on λ^2, hence $k \simeq \pm ik_I$ and $\lambda = \pm ik_I W + m\Omega - \omega + m\Gamma/r^2$, so that the group

$$-k^2 D/\lambda^2 = k_I^2 \left[1 - \frac{4(1 + \Gamma/\Omega r^2)}{\left(\frac{k_I W}{\Omega}\right)^2 + (m - \omega/\Omega + m\Gamma/\Omega r^2)}\right] \qquad (8)$$

must be sufficiently positive. It is schematically plotted as a function of k_I^2 in Fig. 10. For sufficiently large k_I^2, $-k^2 D/\lambda^2$ can be made large whatever the value of $\Gamma/\Omega r^2$, and these large k_I^2 correspond to the pressure disturbances only slightly influenced by rotation.

It appears, however, that there is not an infinite class of attenuated disturbances which have λ/Ω of order unity, unless ω is complex. If $\omega = \omega_R + i\omega_I$ and $k = k_R + ik_I$, we can choose $\omega_I = k_I W$, so λ is real. Then for any value of $\Gamma/\Omega r^2$ there is a value of k_I which will lead to a sufficiently large value of $-k^2 D/\lambda^2$ to insure a solution. But the imaginary ω implies instability, i.e., such a disturbance would grow exponentially in time, Unfortunately for this case the differential equation becomes complex, and no detailed analysis has been carried through. On the basis of this somewhat incomplete argument we tentatively conclude that

b) low frequency (i.e., shear) disturbances of large m are usually temporally unstable, having the form $e^{i(k_r z + m\theta - \omega_R \tau) - k_I(z - \omega\tau)}$

which implies the disturbance is convected from its point of origin, but is exponential in τ at a given value of z.

Summary of Theoretical Results

In summary of this discussion we have the following points for comparison to experiment:

1) Entropy disturbances generated by the blade row should be convected by the mean flow.
2) The "high frequency" pressure field should be only slightly influenced by rotation.
3) Shear disturbances with large m and real k, abd therefore persistent downstream, should occur only in the portion of the annulus where $\Gamma/\Omega r^2$ is small. For the Blowdown Compressor this is roughly the outer half, where the mean tangential velocity approaches a wheel flow.
4) Oscillatory shear disturbances are most likely for small m.
5) For large m and large $\Gamma/\Omega r^2$ there are no steady (in rotor coordinates) shear disturbances, so the wake shedding from the rotor should be intrinsically unsteady.

COMPARISON OF THEORY AND EXPERIMENT

In view of the findings of the previous section the variation of the mean tangential velocity, V(r), with radius should be a controlling factor in the behavior of the shear disturbances downstream of the rotor. As shown in Fig. 6c, it is characterized by a near-free vortex behavior for $r < .82r_t$, and by a near solid body rotation for $r > .82r_t$. The rotor was "designed" to produce a free vortex over the whole annulus. It appears that the excess work in the tip region results from the outward movement of the blade wakes, which have radial Mach numbers as large as 0.7 near mid-span at station 5 and have stagnation pressure ratios as large as 2.0 at that same station.

Oscillatory Flow for $r > .82r_t$

Whatever the origin of V(r), the theory indicates that in the inner region, where $V \propto \Gamma/r$, all disturbances except the entropy should have imaginary or complex axial wave numbers, hence should be attenuated in z. Scrutiny of Figs. 8a to 8e will show that in fact M_r, M_z, M_θ, and p are all relatively uniform at station 6 for $r < .84r_t$. The entropy variation is also fairly weak, but is periodic at blade spacing, indicating convective behavior of the entropy in the inner portion of the annulus, as predicted.

In the outer region, where $V = \Omega r$, the behavior is very different. First, the disturbances of all quantities are very strong at station 6, indicating persistent (oscillatory) phenomena. Secondly, the period is not the blade passing period, but rather about 1.4 times blade passing period. Comparing Figs. 8d and 8e we see that zones of strong inward and outward flow exist, together with alternate large and small tangential flow, the maxima of the latter being near the nodes of the former. This describes a cellular vortex flow of the type which occurs between coaxial rotating cylinders under some conditions of radial circulation variation. It is consistent with the prediction of the previous section, which of course includes the physical phenomena that give rise to a cellular flow. A qualitative demonstration of this can be given by modeling the outer region by a wheel flow, to which the relatively simple Eq. (6) applies. The velocities are given by

$$u = \frac{i}{\lambda^2 - 4\Omega^2} \left(\frac{\lambda}{R}\frac{dp}{dr} + \frac{2m\Omega}{Rr} p\right) \tag{9}$$

$$v = \frac{1}{\lambda^2 - 4\Omega^2} \left(\frac{2\Omega}{R}\frac{dp}{dr} - \frac{m}{Rr} p\right) \tag{10}$$

$$w = \frac{k}{\lambda R} p \tag{11}$$

where $p = Z_m(\mu r)$, the general cylindrical harmonic. The argument μ is connected to λ by[3]

$$(\mu r_t)^2 = \left(\frac{\Omega r_t}{w}\right)^2 \left[4 - \left(\frac{\lambda}{\Omega}\right)^2\right] \left[1 + \left(\frac{\omega}{\Omega} - m\right)\frac{\Omega}{\lambda}\right]^2 \tag{12}$$

To determine m and μr_t one should match some set of boundary conditions at the inner and outer radii. For present purposes we simply observe that the first mode is likely to have a half wave-length in $r\theta$ about equal to that in r, since this allows $u = 0$ at r_t and at $.82\ r_t$, where the oscillation terminates. Thus we expect

$$\frac{2\pi(.91\ r_t)}{m} \simeq 2(.18\ r_t)$$

where $.91\ r_t$ is the mean radius of the outer region. This gives $m = 15.9$, and we note that $23/1.4 \simeq 16.4$, the 1.4 being the number of blade passing periods characterizing the disturbance in the outer region. Certainly this is a bit fortuitous! Now $\omega/\Omega \simeq 16\ M_t/\bar{M}_{\theta t} = 42$ where M_t is the tangential Mach number of the rotor, and $\omega/\Omega - m = 42 - 16 = 26$. Estimating $\mu r_t \simeq 26$, which is the second zero of $J_{16}(\mu r)$, we then find $\lambda/\Omega = 0.77$ or -0.73. The variations of the radial, tangential, and axial velocities are then readily found from Eqs. (9) to (11). For comparison to the data it is convenient to express them in terms of Mach number variations. Thus, we write for example

$$\frac{u\Omega R r_t}{p} = \frac{\gamma u \Omega r_t}{\gamma R T} = \gamma \tilde{M}_r \bar{M}_{\theta t}$$

where $\tilde{M}_r$ is the radial Mach number perturbation and $\bar{M}_{\theta t}$ is the mean swirl Mach number at the tip (about 0.45). The predictions of the theory are given in this form in Fig. 11 for $\lambda/\Omega = 0.77$, which gives the best match to the data of the two possible values of λ/Ω.

Note first that the data are restricted to the region $r < .93\ r_t$. Within this range the signs and phases of u, v, w, and p are all mutually consistent with the theory. That is, where p/P is positive, $\tilde{M}_z$ is negative, $\tilde{M}_\theta$ is negative, and M_r is negative. From the theory, $\tilde{M}_r \propto i\tilde{M}_\theta$, i.e., it is shifted <u>ahead</u> $\pi/2$ in $m\theta$, so that an event in $\tilde{M}_r$ should occur $\pi/2$ earlier in ωt than the corresponding event in $m\theta$, and comparison of Figs. 8d and 8e shows this is approximately true.

There is not good quantitative agreement as to the relative magnitudes of $\tilde{M}_z$, p/P and the pair $\tilde{M}_r$ and $\tilde{M}_\theta$, but this is not surprising as the model is very crude.

<u>Harmonic Content of Downstream Pressure Field</u>

One striking feature of Fig. 11 is that p/P is predicted to be small at r_t, where of course $\tilde{M}_r$ was specified to be zero. This is in contrast to acoustical theories, where generally pressure maxima occur at velocity nodes.

A series of measurements of static pressure was carried out in the Blowdown Compressor by Stephens[8] at stations 5, 6, and 7. Measurements were made both with flush wall static transducers and with a survey probe. The survey probe, when positioned at about .90 to .95 r_t showed a very strong spectral peak at a frequency which shifted from blade passing ($m = 23$) at station 5 to higher values at stations 6 and 7. These spectra are shown in Fig. 12a. Note that the strength of the peak actually increases with distance from the rotor!

In contrast, the flush mounted wall static transducer shows a rapidly decaying tone at $m = 23$, as shown in Fig. 12b. We infer that the latter is due to the elliptic pressure field of the rotor, which has its radial maximum at r_t, where $u = 0$, while the strong peaks of Fig. 12a are due to the pressure field of the oscillatory shear flow, which according to Fig. 11 should not be detected at r_t, but should be strong for $.82\ r_t < r < r_t$.

The reason for the upward shift in this frequency is not yet clear, but note that the data does not include the region very near r_t. It may be that a secondary shear structure exists there.

Harmonic Content of Upstream Pressure Field

Measurements of the upstream pressure field of the rotor showed a well developed duct-modal structure with dominant harmonics at m = 7 and m = 16.[4] Aside from the dominance of these two "tones", the upstream sound field was typical of the "combination tone" field of a transonic fan. It now seems clear that the strong m = 16 tone is excited by the cellular flow in the downstream annulus. Perhaps the m = 7 is in fact a combination tone of m = 23 and m = 16?

Unsteadiness

By careful examination of the wake from a single blade in successive passes by the probe we conclude that for this rotor the flow in rotor coordinates is unsteady. It seems to be true in general that the wake shedding from the blades of highly loaded rotors is aperiodic with blade passing, and in fact probably quite random. A possible explanation for this lies in the lack of existence of a set of stable low frequency (shear) disturbances for flows where $\Gamma/\Omega r^2 > 1$. The theory predicts that shear disturbances should be unstable, i.e., should grow exponentially in time for such a situation. Evidently a nonlinear oscillation results from the instability.

REFERENCES

1. Epstein, A. H., *Quantitative Density Visualization in a Transonic Rotor*, AIAA Paper No. 75-24, 1975.

2. Lakshminarayana, B., and Poncet, A., *A Method of Measuring Three-Dimensional Wakes in Turbomachinery* J. Fluids Engr., June 1974.

3. Kerrebrock, J. L., *Waves and Wakes in Turbomachine Annuli with Swirl*, AIAA Paper No. 74-87, 1974.

4. Kerrebrock, J. L., Epstein, A. H., Haines, D. M., and Thompkins, W. T., *The M.I.T. Blowdown Compressor Facility*, J. Engr. for Power, 96, 4, Oct. 1974, pp. 394-405.

5. Epstein, A. H., *Quantitative Density Visualization in a Transonic Compressor Rotor*, Ph.D. Thesis, Mass. Institute of Technology, Sept. 1975.

6. Kovasznay, L.S.G., J. Aero. Sci., 20, 10, Oct. 1953.

7. Yousefian, V., *Propagation of Disturbances in Compressor Annuli with Solid Body Rotation and Throughflow*, Ph.D. Thesis, Mass. Institute of Technology, June 1975.

8. Stephens, H. E., III, *Wake Behavior Downstream of a Transonic Compressor Rotor*, S.M. Thesis, Mass. Institute of Technology, Sept. 1974.

ACKNOWLEDGMENTS

The experimental portion of this work was supported by the NASA Lewis Research Center under Grant NGL 22-009-383, supervised by Mr. W. D. McNally. The theoretical work was supported by Pratt & Whitney Aircraft Division, United Technology Corporation. General support of the Gas Turbine Laboratory is provided by the General Electric Company.

The authors are indebted to Mr. Alan H. Epstein, who has contributed much to the Blowdown Compressor program, to Mr. Harry E. Stephens, III, and to Mr. Thorwald Christensen, whose expertise has been essential.

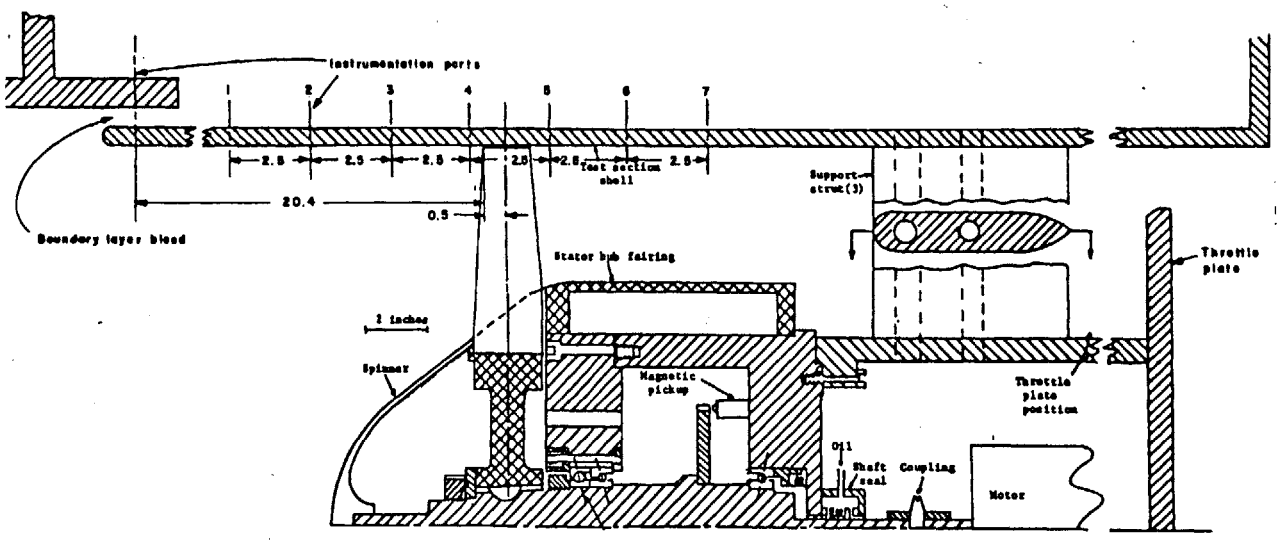

Figure 1: Sketch of Blowdown Compressor Facility showing Rotor Placement and Instrumentation Ports

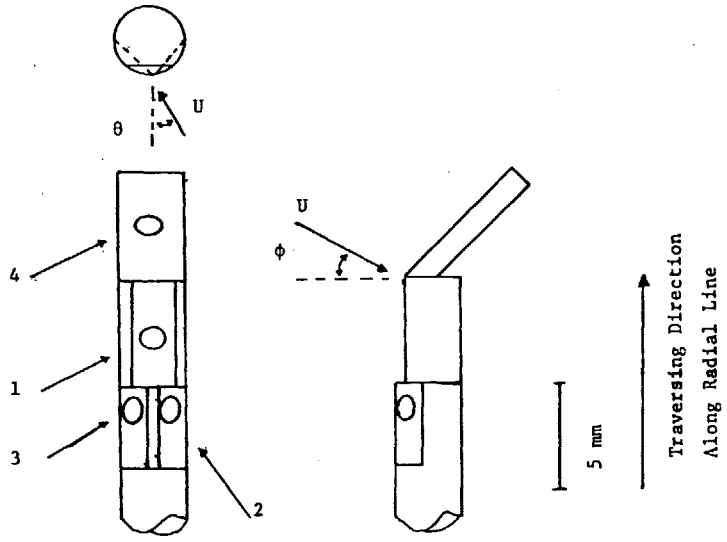

Figure 2: Sketch of Four-Diaphragm Probe Showing Air Angle Definitions

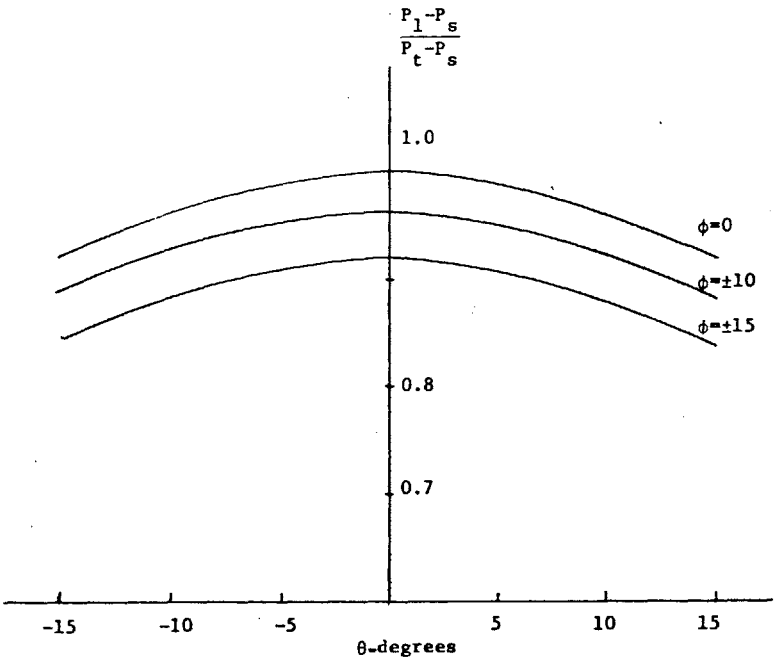

Figure 3a: Four-Diaphragm Probe Calibration
Pressure Recovery for Diaphragm 1

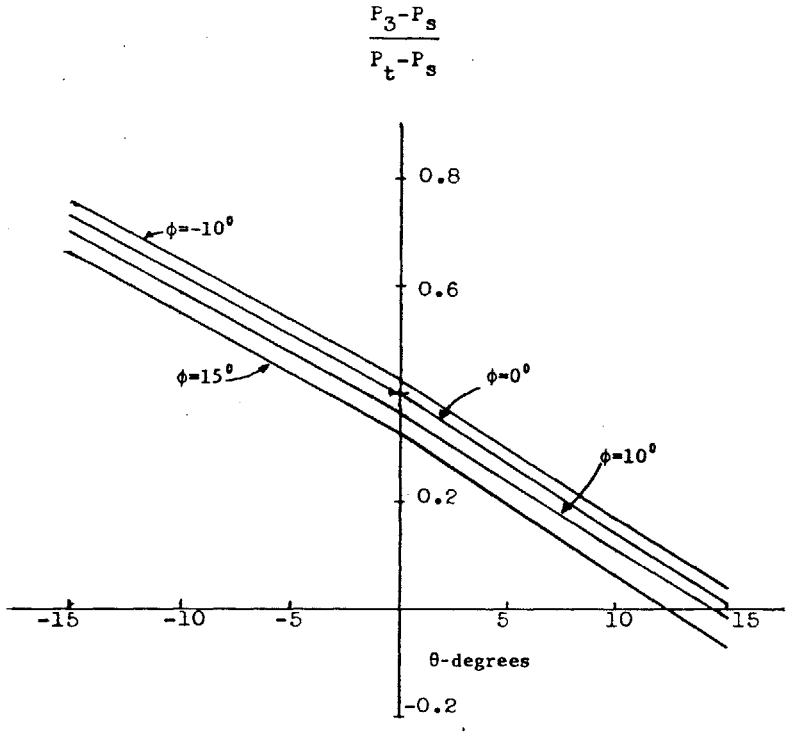

Figure 3b: Four-Diaphragm Probe Calibration
Pressure Recovery for Diaphragm 3

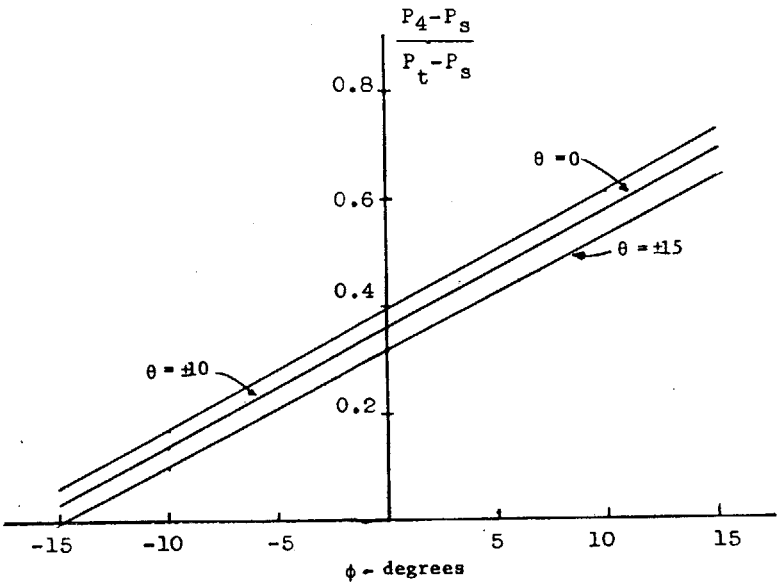

Figure 3c: Four-Diaphragm Probe Calibration
Pressure Recovery for Diaphragm 4

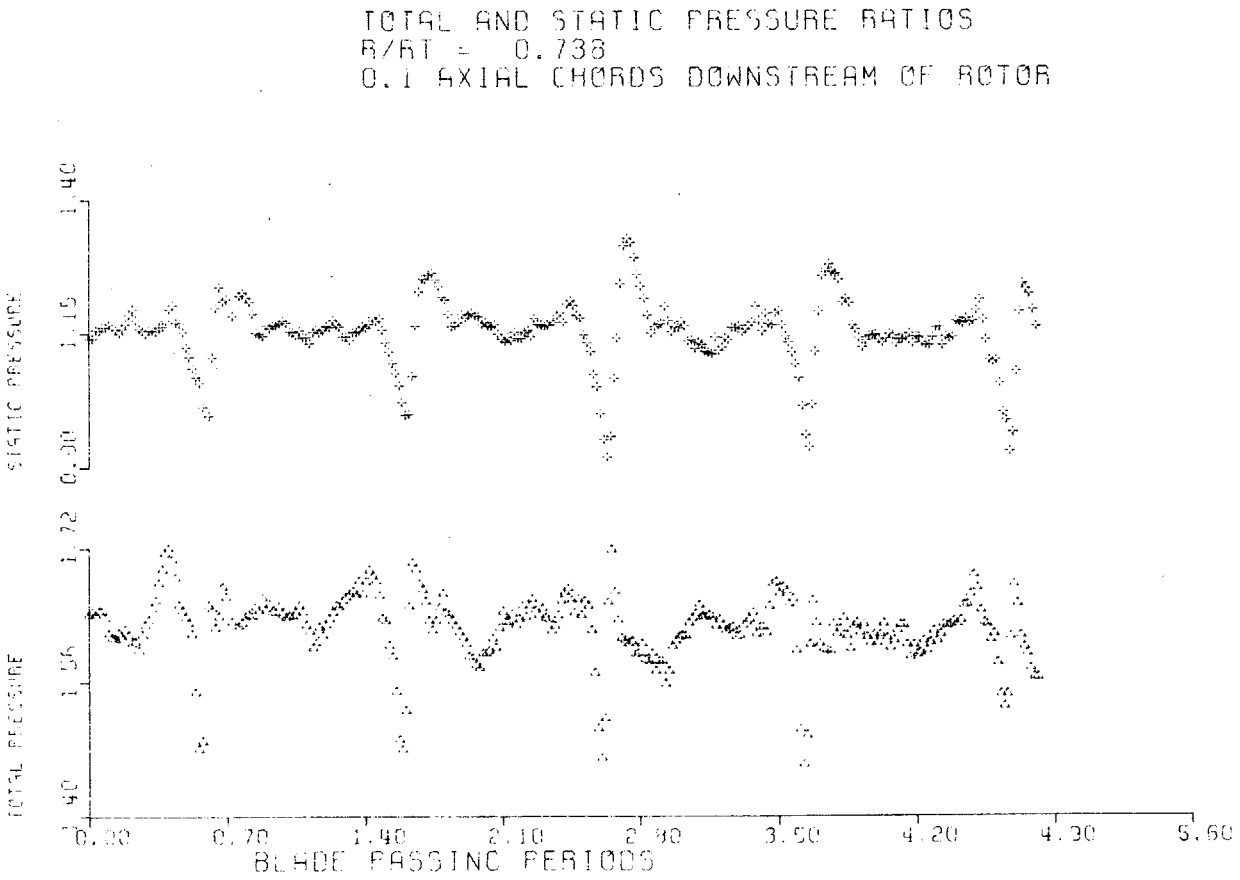

Figure 4a

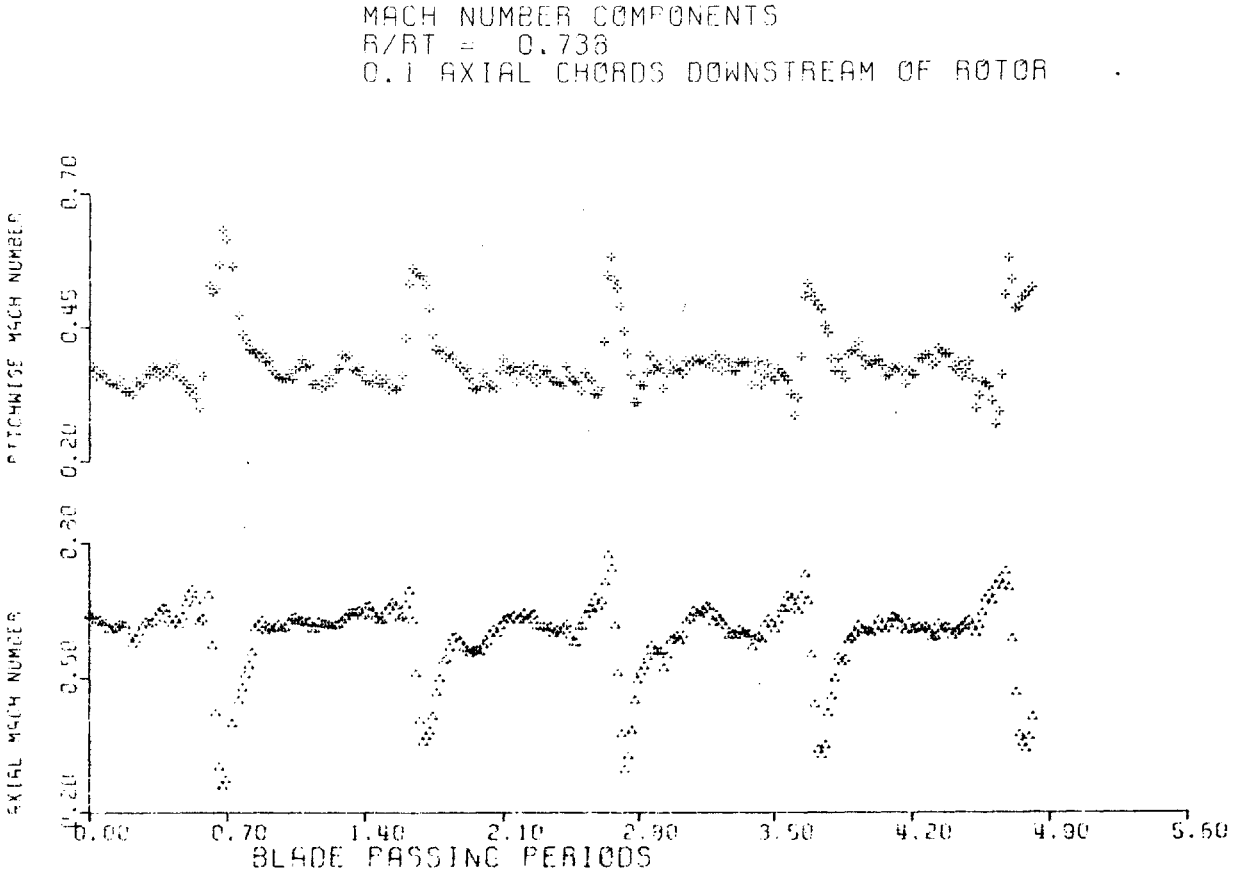

Figure 4b

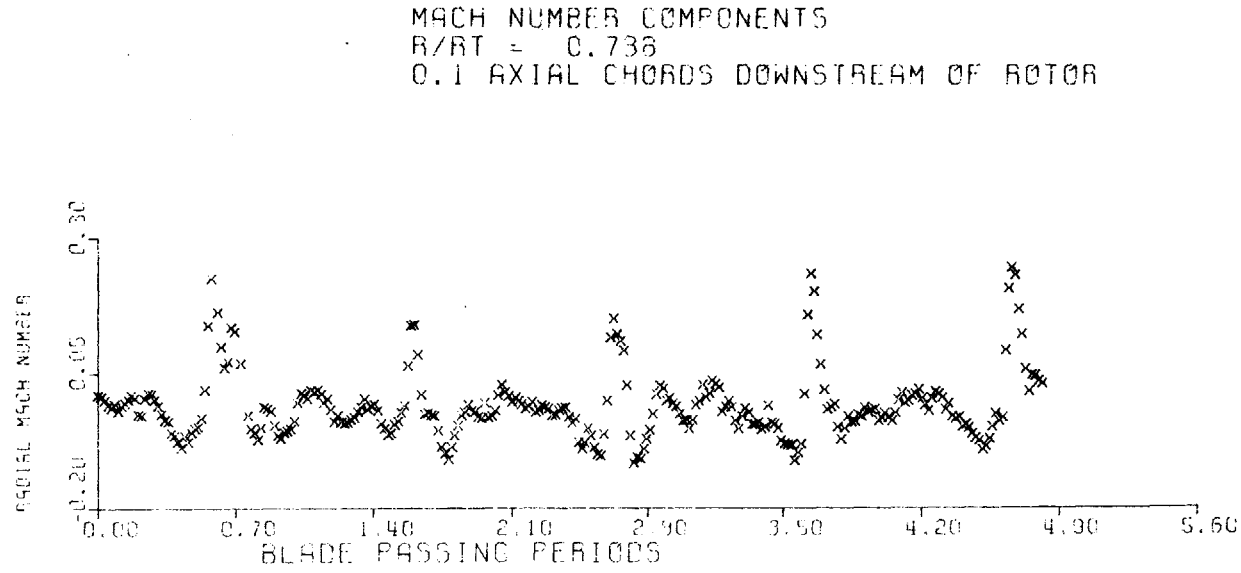

Figure 4c

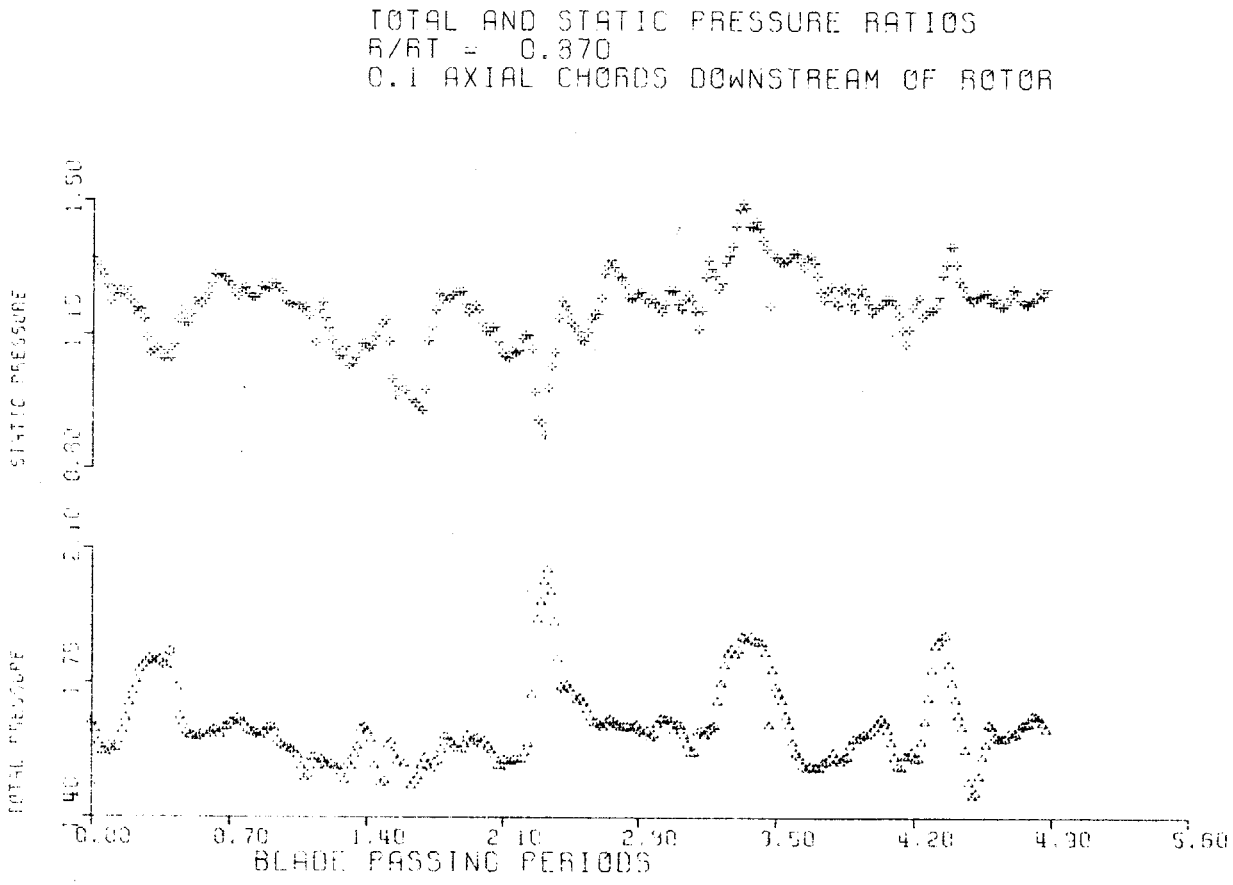

Figure 5

Time Averaged Total Pressure and Total Tempetature ratios

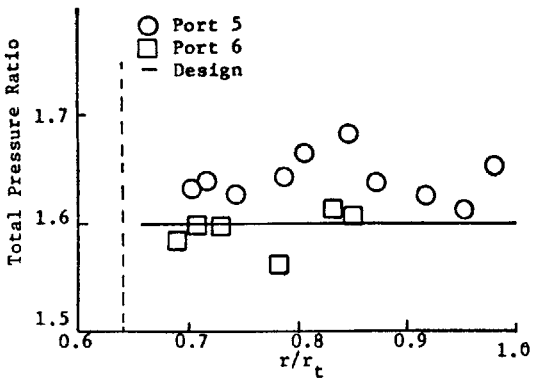

Figure 6a

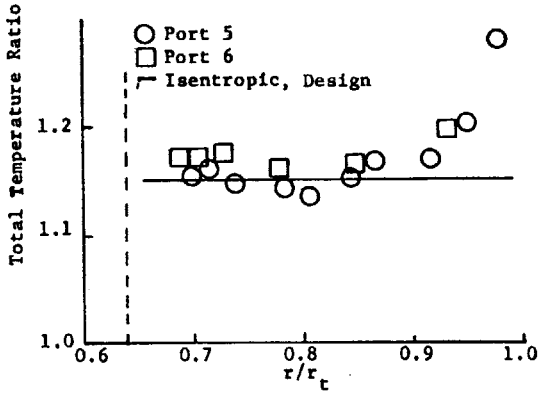

Figure 6b

Time Averaged Mach Number Profiles

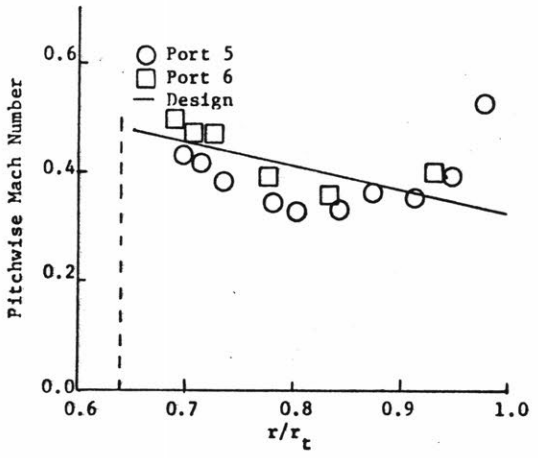

Figure 6c

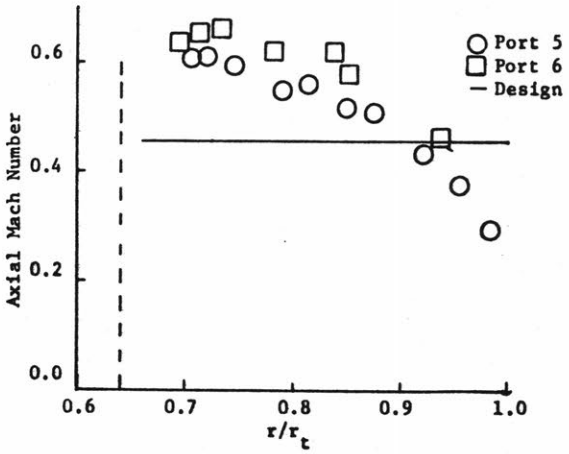

Figure 6d

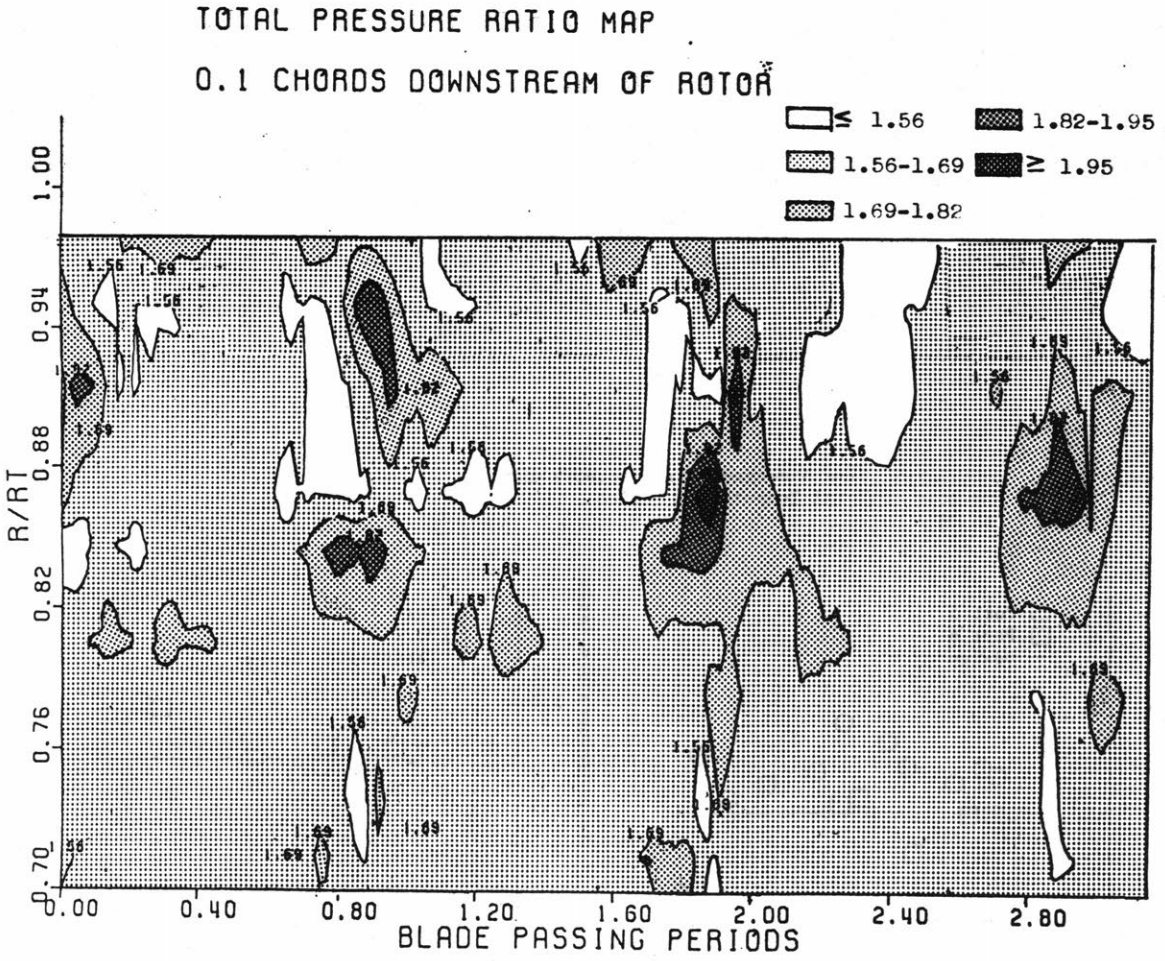

Figure 7a

Figure 7b: STATIC PRESSURE RATIO MAP

0.1 CHORDS DOWNSTREAM OF ROTOR

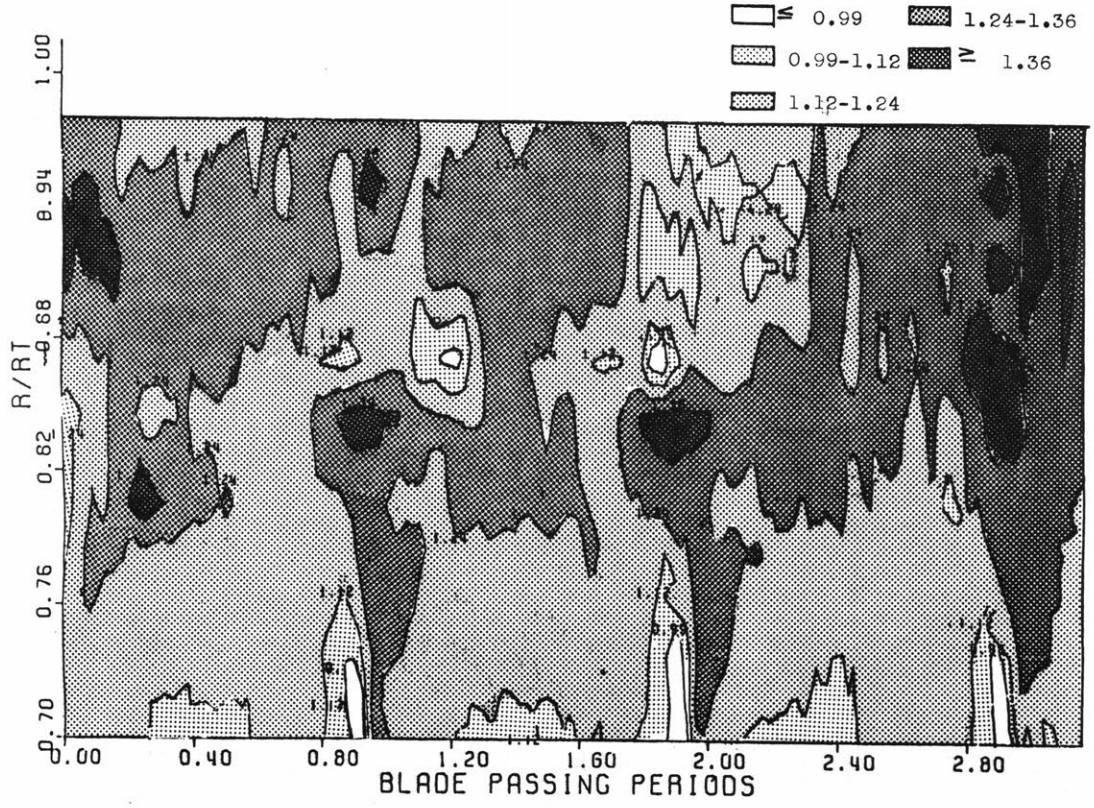

Figure 7c: ENTROPY RISE MAP

0.1 CHORDS DOWNSTREAM OF ROTOR

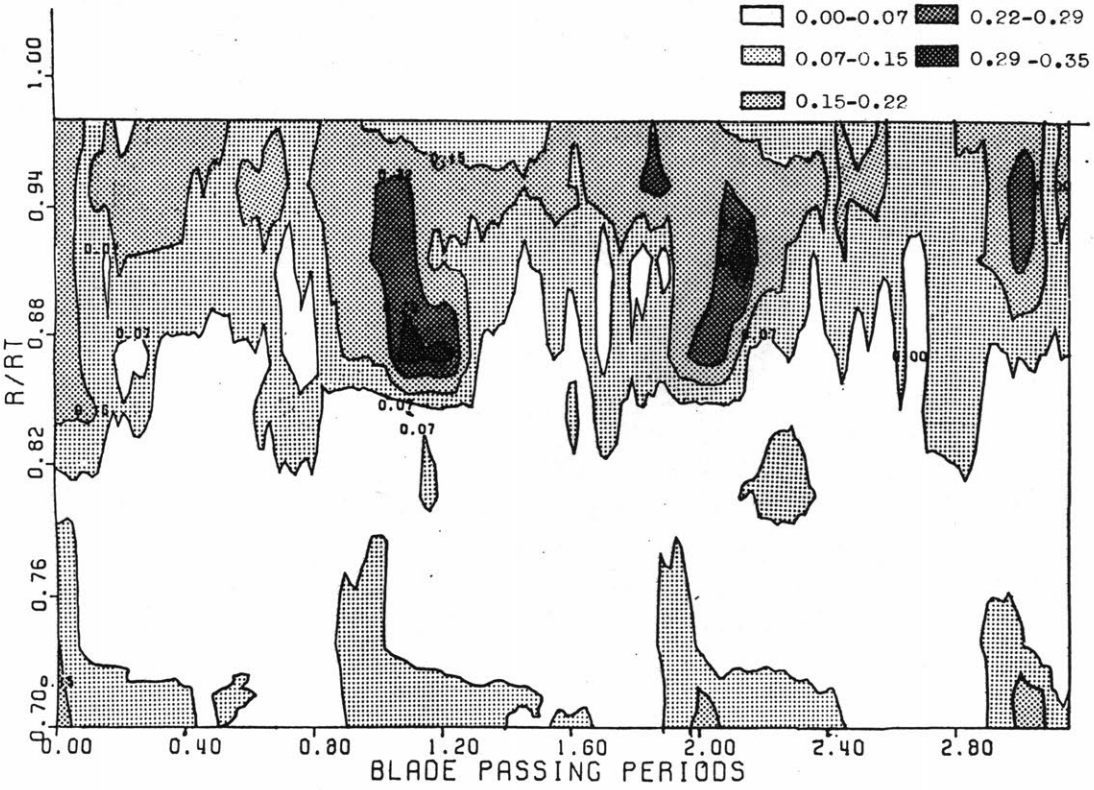

Figure 7d: AXIAL MACH NUMBER MAP

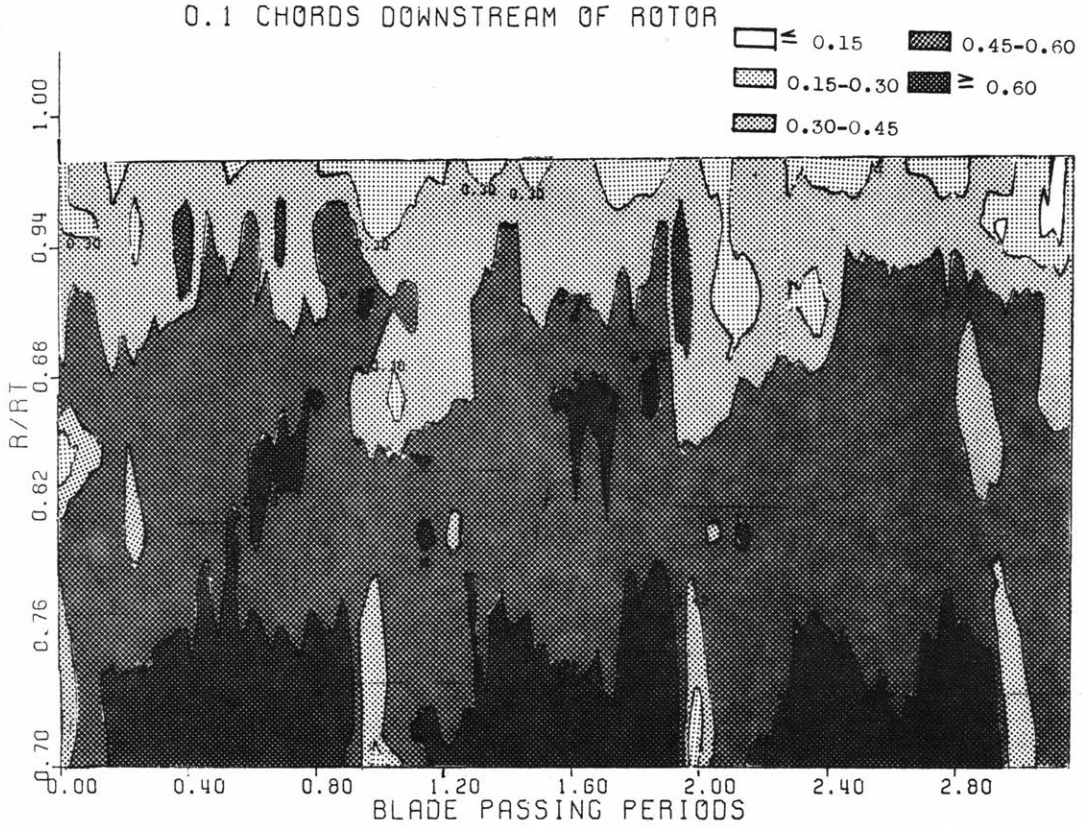

Figure 7e: PITCHWISE MACH NUMBER MAP

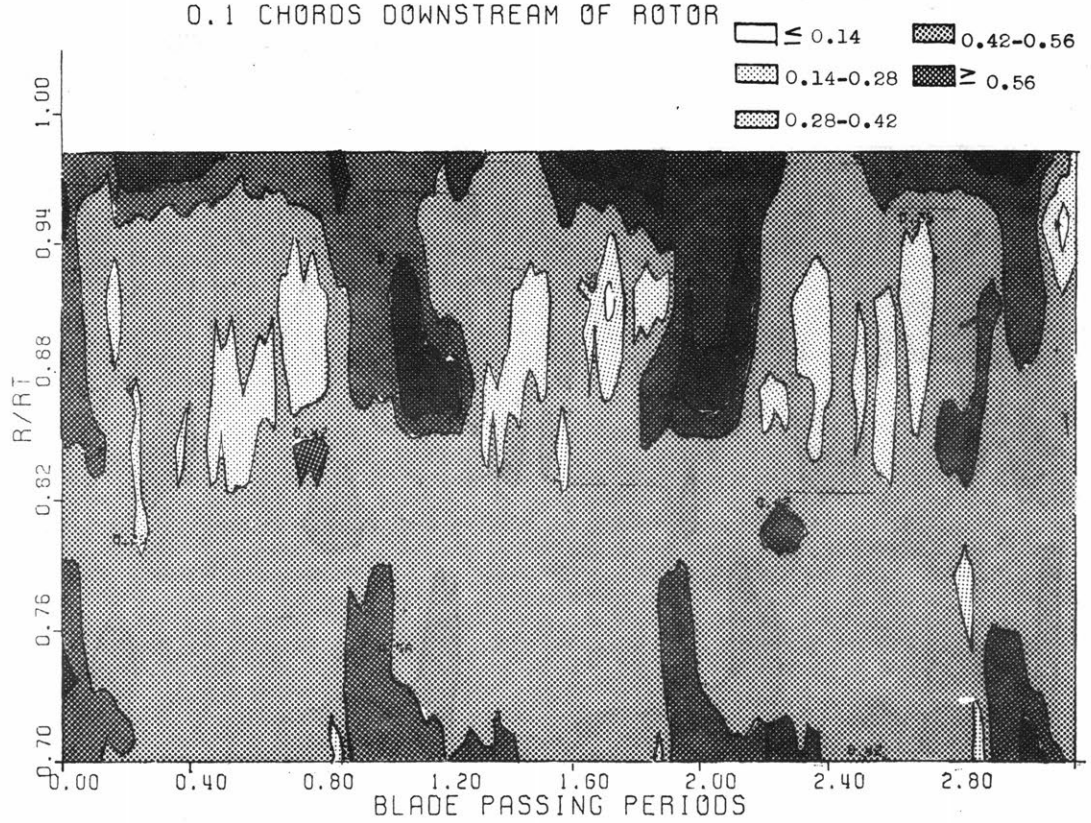

Figure 7f: RADIAL MACH NUMBER MAP

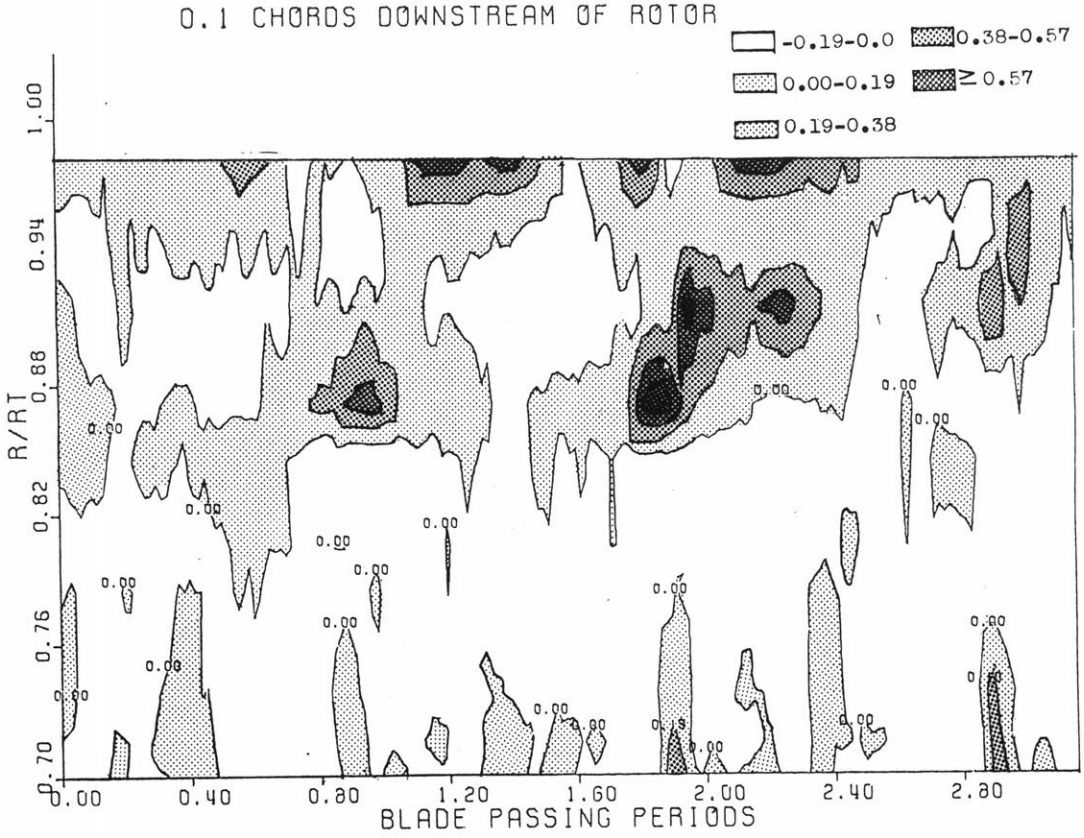

Figure 7g: TOTAL TEMPERATURE RATIO MAP

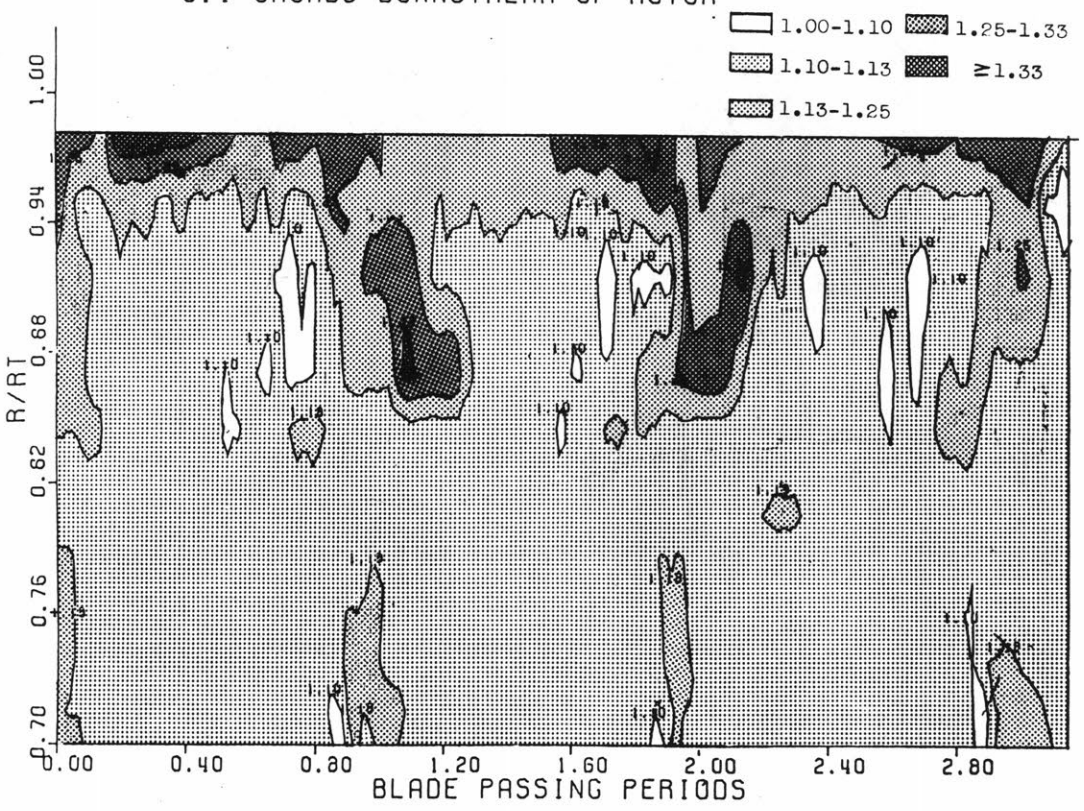

Figure 8a: ENTROPY RISE MAP

1.0 CHORDS DOWNSTREAM OF ROTOR

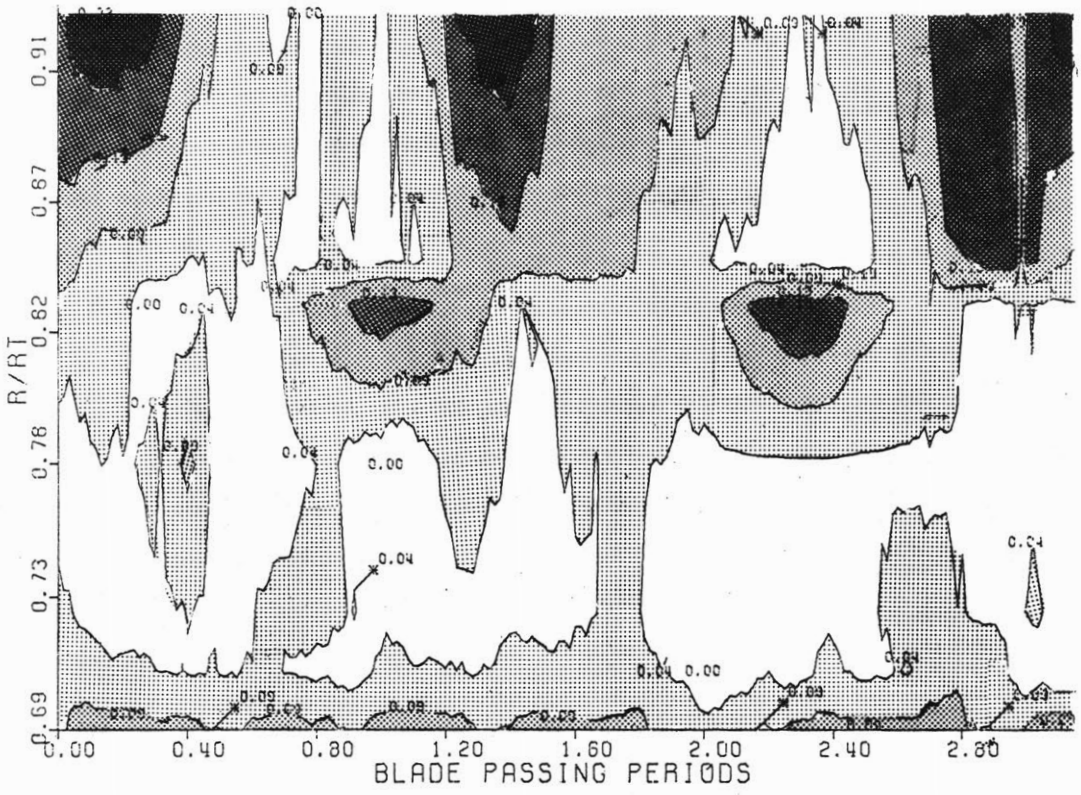

Figure 8b: STATIC PRESSURE RATIO MAP

1.0 CHORDS DOWNSTREAM OF ROTOR

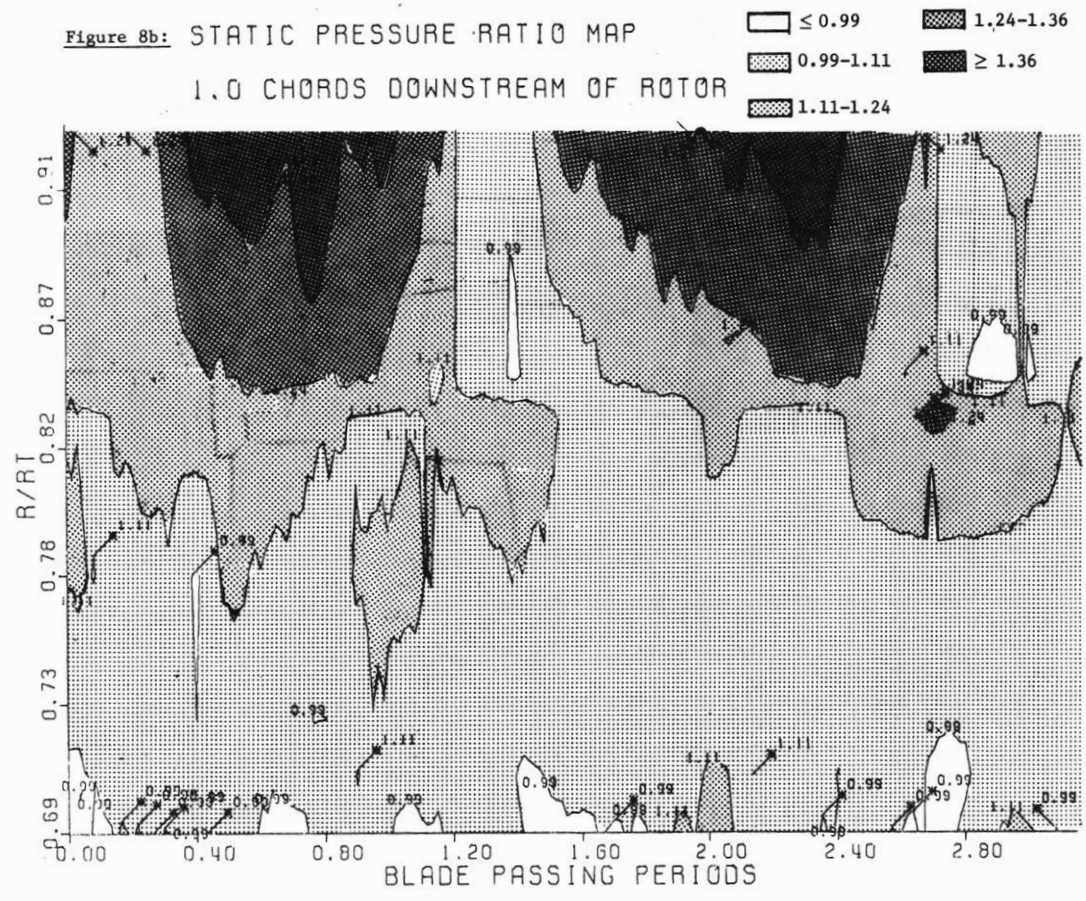

Figure 8c: AXIAL MACH NUMBER MAP

1.0 CHORDS DOWNSTREAM OF ROTOR

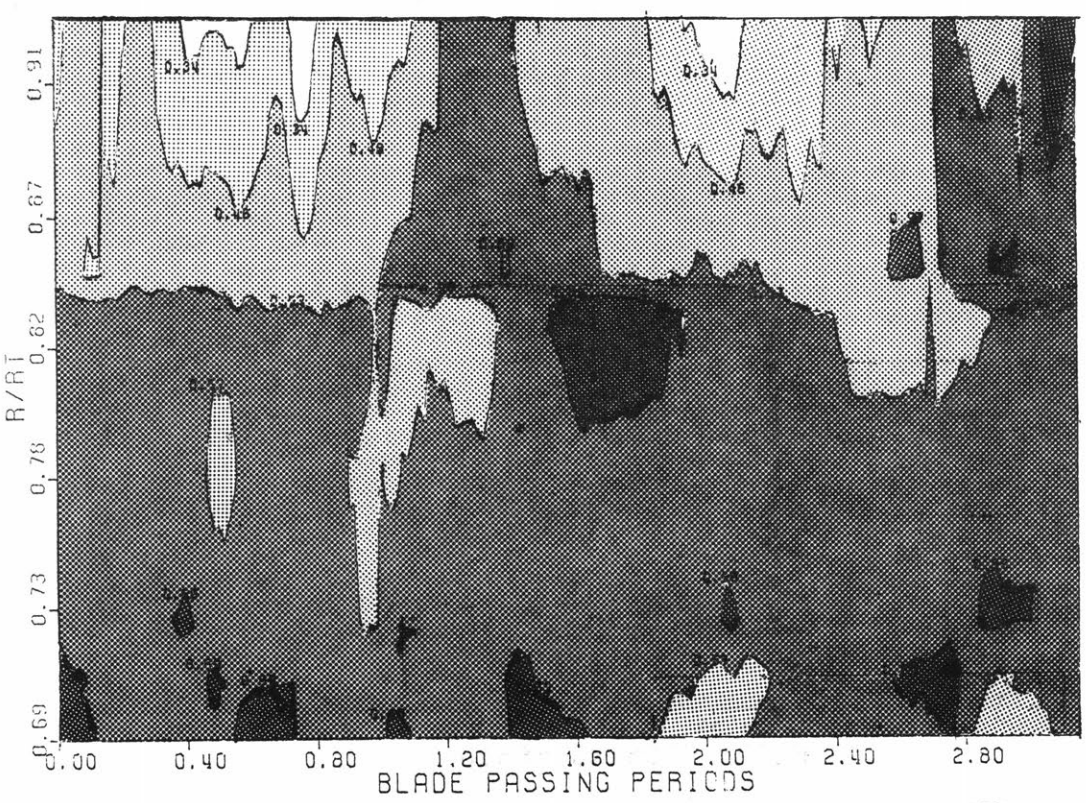

Figure 8d: PITCHWISE MACH NUMBER MAP

1.0 CHORDS DOWNSTREAM OF ROTOR

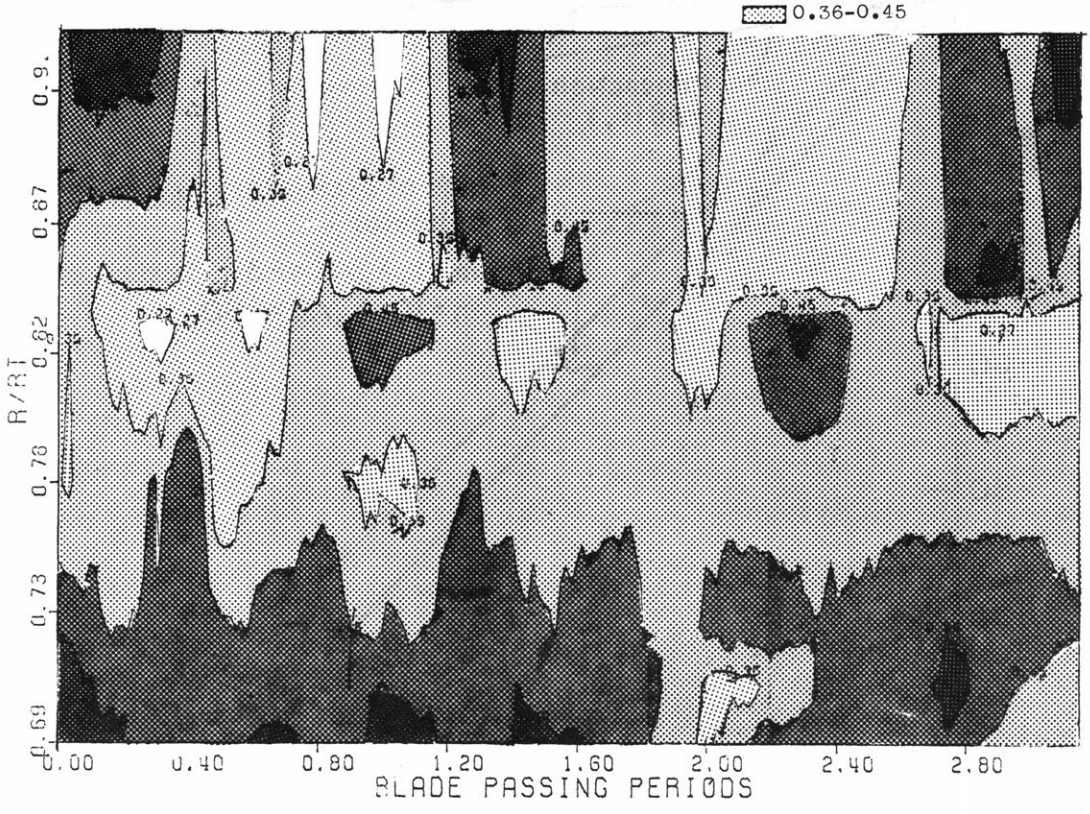

Figure 8e: RADIAL MACH NUMBER MAP

1.0 CHORDS DOWNSTREAM OF ROTOR

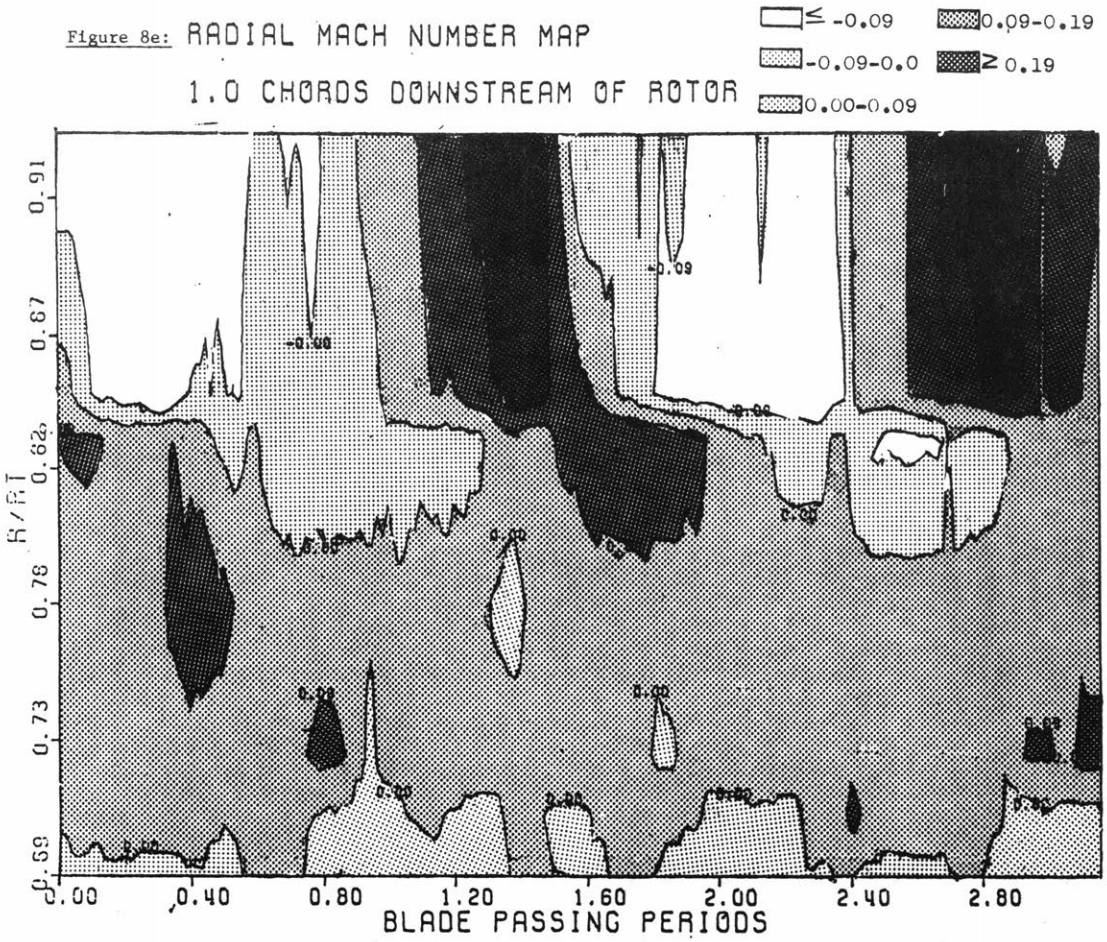

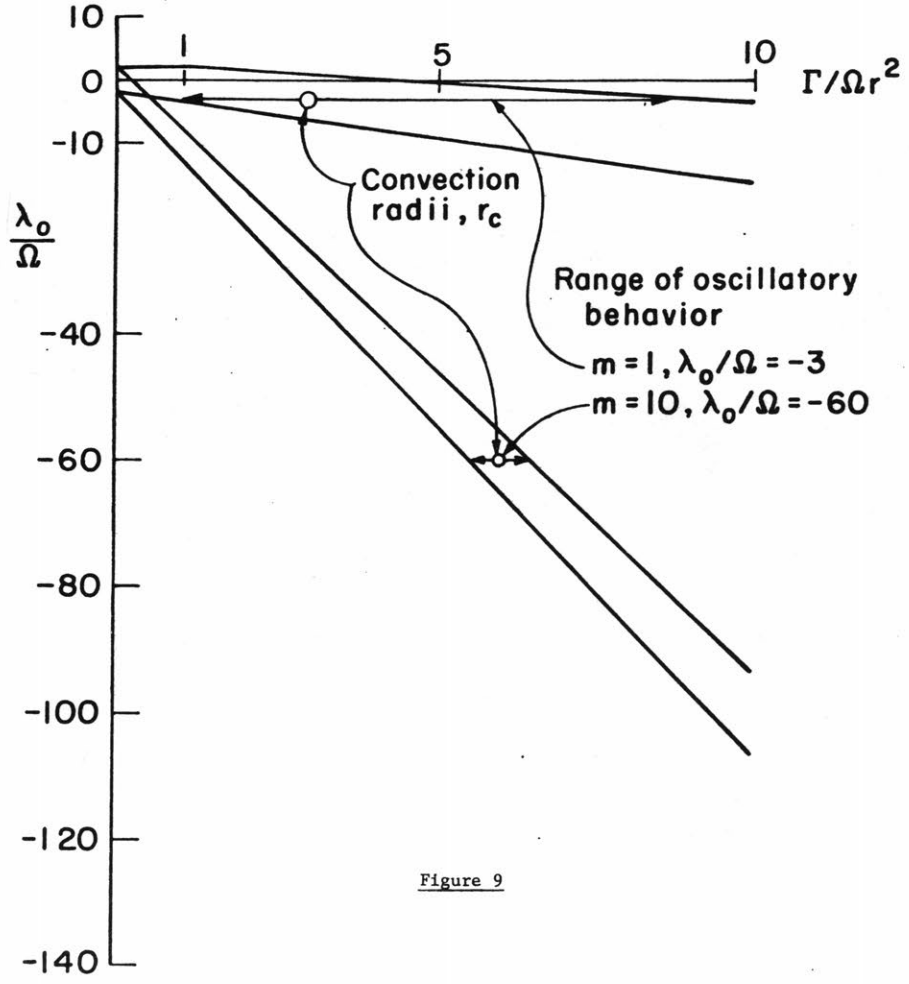

Figure 9

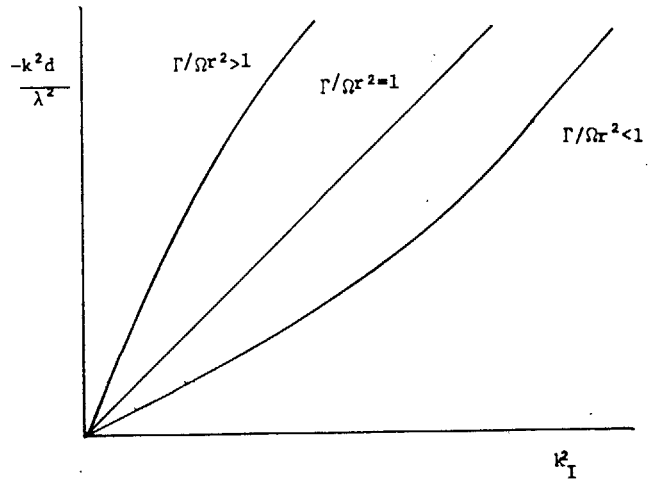

Figure 10

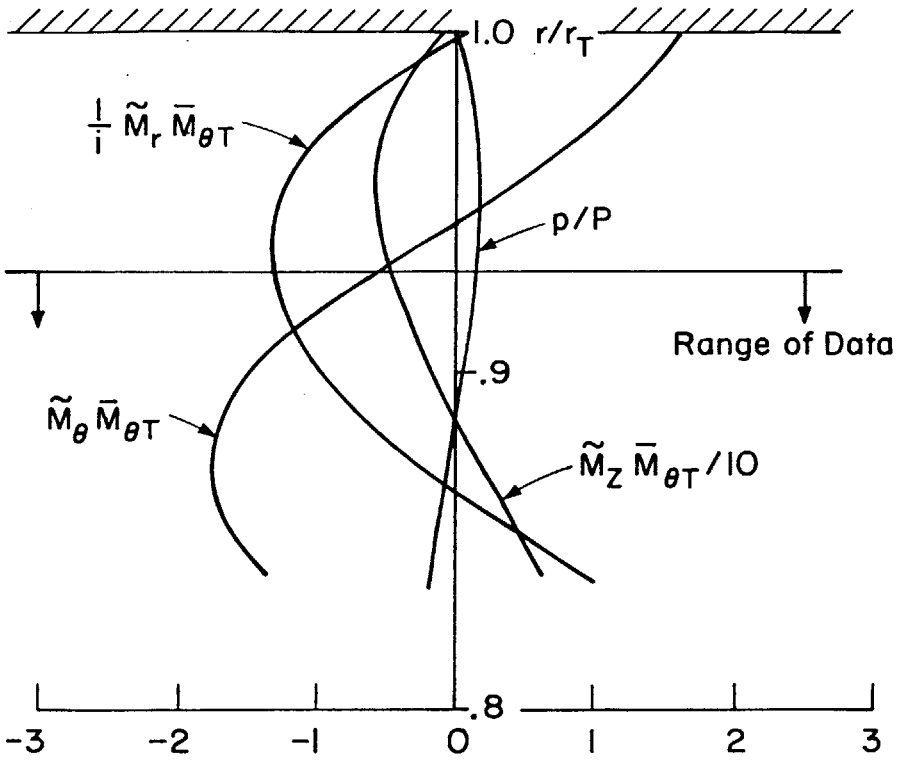

Figure 11

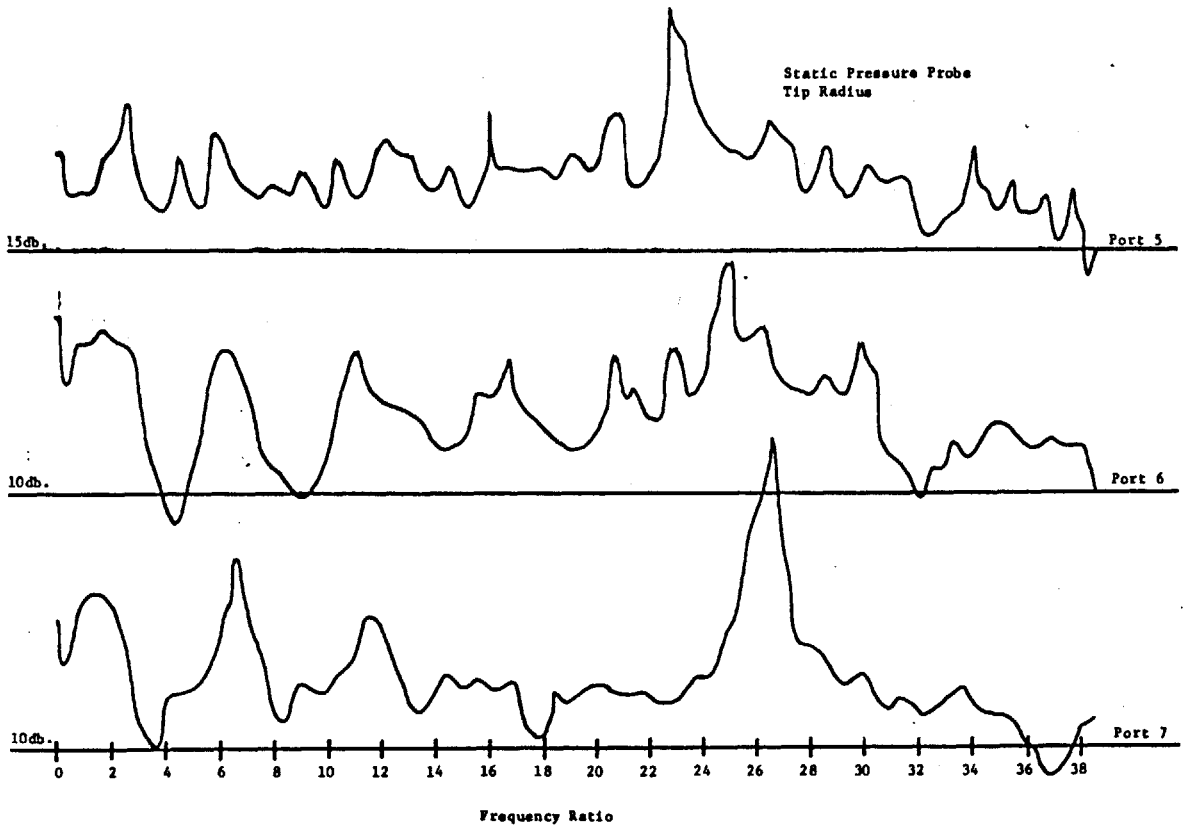

Figure 12a

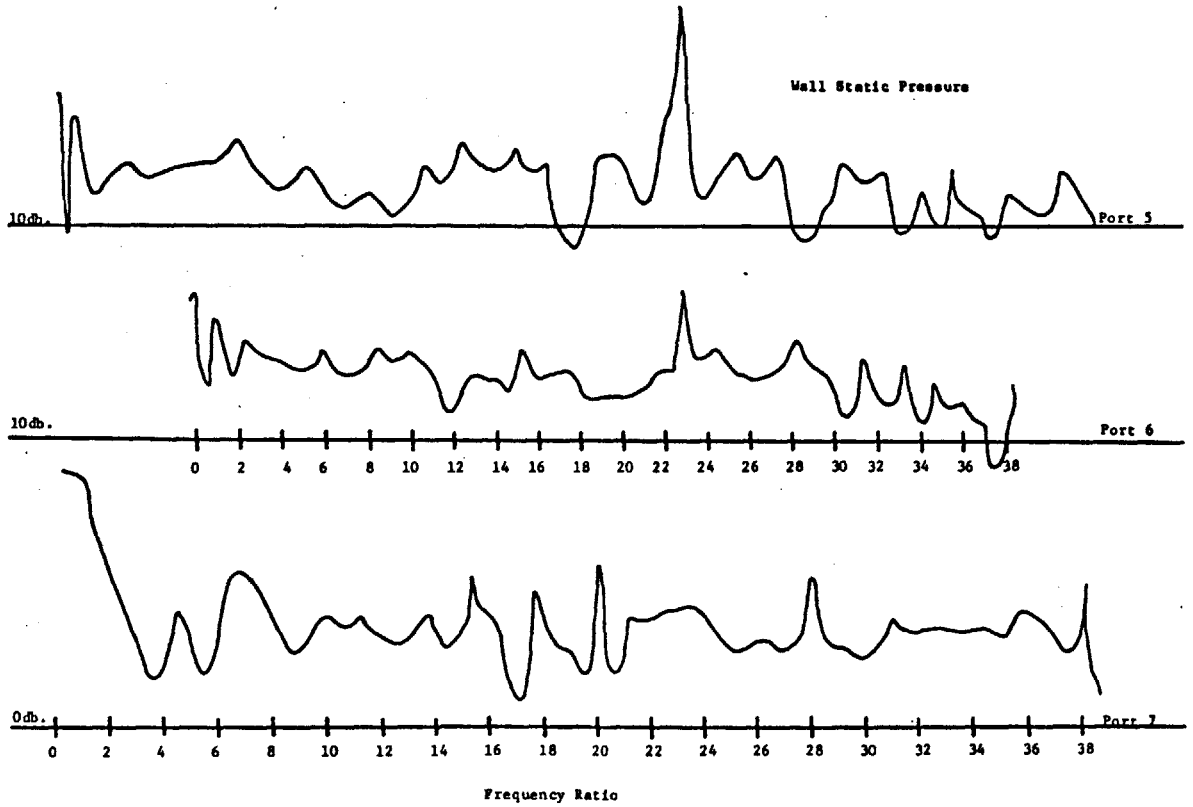

Figure 12b